

A STUDY OF NON LINEAR  
EFFECTS IN MINERALISED ROCKS

BY  
ROBERT M. S. WHITE

Thesis submitted in partial fulfillment for the degree of Master of Science at  
Macquarie University.

AUGUST 1974

## ABSTRACT

Methods usually employed in geophysical search for minerals make use of very few of the electrical properties of these minerals.

This present study looked at the semi-conducting properties of certain electronically conducting minerals.

Equipment was developed to measure these properties in the laboratory. The method developed used two exciting frequencies and detected intermodulation products caused by nonlinear conduction.

Of the samples tested the non-mineralized cores were linear within the limits of the measuring apparatus. The mineralized samples however did show nonlinearity of conduction. The nonlinearity was greatly enhanced by the use of a direct current bias. The magnitude of the signals obtained using the direct current bias may enable the method to be used in the field.

# CONTENT

<b>1. INTRODUCTION.....</b>	<b>5</b>
1.1 ELECTRICAL PROSPECTING. ....	5
1.2 ELECTRICAL CONDUCTION IN ROCKS.....	9
1.3 NON-LINEAR CONDUCTION.....	14
1.4 PREVIOUS WORK.....	20
<b>2. SEMI-CONDUCTION.....</b>	<b>23</b>
2.1 THE MECHANISM OF CONDUCTION IN SEMI-CONDUCTORS.....	23
2.2 SEMI-CONDUCTING MINERALS.....	28
<b>3. EXPERIMENTAL METHODS AND RESULTS.....</b>	<b>31</b>
3.1 CURRENT DENSITIES.....	31
3.2 SINGLE FREQUENCY METHOD OF MEASURING NON-LINEAR CONDUCTION.....	34
3.3 METHOD OF MEASUREMENT.....	37
3.4 RESULTS.....	41
3.5 DOUBLE FREQUENCY METHOD OF MEASURING NON-LINEAR CONDUCTION.....	48
3.6 METHOD OF MEASUREMENT.....	52
3.7 RESULTS.....	57
<b>4. DISCUSSION OF RESULTS.....</b>	<b>66</b>
<b>5. CONCLUSION.....</b>	<b>76</b>
<b>6. FUTURE WORK.....</b>	<b>78</b>
<b>APPENDIX A.....</b>	<b>79</b>
<b>APPENDIX B.....</b>	<b>81</b>
<b>BIBLIOGRAPHY.....</b>	<b>84</b>

## FIGURES

<b>FIGURE 1 POTENTIAL DISTRIBUTION ABOUT A SULPHIDE GRAIN.</b> .....	11
<b>FIGURE 2 IP EQUIVALENT CIRCUIT.</b> .....	12
<b>FIGURE 3 RESISTIVITY VS TEMPERATURE FOR SEMICONDUCTORS.</b> .....	23
<b>FIGURE 4. SCHEMATIC DIAGRAM SHOWING ELECTRON LEVELS.</b> .....	25
<b>FIGURE 5 SIMPLIFIED CONDUCTION PATH IN MINERALISED ROCK.</b> .....	32
<b>FIGURE 6 MODEL USED FOR CURRENT DENSITY CALCULATIONS.</b> .....	33
<b>FIGURE 7 DISTORTION DUE TO NON LINEAR ELEMENT.</b> .....	34
<b>FIGURE 8 DISTORTION AFTER REMOVAL OF LINEAR ELEMENT.</b> .....	34
<b>FIGURE 9 IP BRIDGE USED TO REMOVE LINEAR ELEMENT.</b> .....	36
<b>FIGURE 10 CELL USED IN MEASUREMENTS.</b> .....	38
<b>FIGURE 11. SCHEMATIC OF CIRCUIT USED IN MEASUREMENTS.</b> .....	39
<b>FIGURE 12. VOLTAGE VS CURRENT, DRY CORE, 10UA.</b> .....	42
<b>FIGURE 13. VOLTAGE VS CURRENT, SATURATED CORE, 5UA.</b> .....	42
<b>FIGURE 14. VOLTAGE VS CURRENT, SATURATED CORE, HIGH CURRENT DENSITY, 100UA.</b> ....	43
<b>FIGURE 15. VOLTAGE VS CURRENT, DRY CORE, 10UA.</b> .....	45
<b>FIGURE 16. VOLTAGE VS CURRENT, SATURATED CORE, 50UA.</b> .....	45
<b>FIGURE 17. VOLTAGE VS CURRENT, DRY CORE, 100UA.</b> .....	45
<b>FIGURE 18. VOLTAGE “STEPPING” OBSERVED IN CURVES.</b> .....	46
<b>FIGURE 19. CIRCUIT USED TO TEST THE WAVE ANALYSER.</b> .....	53
<b>FIGURE 20. MODIFIED MEASURING CIRCUIT.</b> .....	54
<b>FIGURE 21. SCHEMATICS OF THE CIRCUITS USED FOR ALL SUBSEQUENT TESTING.</b> .....	56
<b>FIGURE 22. WAVEFORM USED IN EXCITING THE ROCK SAMPLES</b> .....	58
<b>FIGURE 23. FIRST HARMONIC VERSES DC BIAS CHANGE.</b> .....	60
<b>FIGURE 24. FIRST HARMONIC VERSES DC BIAS CHANGE, AT AC HIGHER CURRENTS.</b> .....	62
<b>FIGURE 25. FIRST HARMONIC, CONSTANT AC AND VARIABLE BIAS.</b> .....	64
<b>FIGURE 26. POTENTIAL DISTRIBUTION ACROSS N - N<sup>+</sup> JUNCTION.</b> .....	67
<b>FIGURE 27. ENERGY BANDS FOR SHOTTKY DIODES.</b> .....	68
<b>FIGURE 28. ENERGY BANDS FOR SHOTTKY DIODES WITH REVERSE BIAS.</b> .....	68
<b>FIGURE 29. VOLTAGE/CURRENT CHARACTERISTICS FOR DIFFERENT DOPING LEVELS.</b> .....	71
<b>FIGURE 30. FIRST HARMONIC VERSES DC BIAS CHANGE, AT HIGHER DC &amp; AC CURRENTS.</b> ..	72
<b>FIGURE 31. VOLTAGE CURRENT CHARACTERISTICS OF A P-N JUNCTION.</b> .....	74

# 1. INTRODUCTION

## 1.1 ELECTRICAL PROSPECTING.

During 1912 the Schlumberger Brothers did surveys in France with sets of electrodes and wires measuring electrical resistivities of rocks in an endeavour to determine what lay under the surface. Since this time the general resistivity method has been refined and changed in an attempt to gain more accurate knowledge of subsurface conduction and its meaning.

Probably the simplest electrical method is the self potential method where two electrodes are placed in the ground and natural voltages that exist in the crust are measured. These measurements are usually D.C. and measure voltages caused by ore bodies, streaming, potentials etc. A more refined method uses the measurement of telluric voltages in an attempt to determine conductivity and depth.

These potential methods have the advantage that no artificial source is needed. They have the interpretational disadvantage that there is no control over the source.

To gain greater resolving power, an artificial source can be introduced into the ground via 2 electrodes, while a second pair is used to measure the resulting potential gradient. By moving these electrodes in relation to one another a great deal can be learnt about the variations of the resistivity both vertically and horizontally.

From Ohms law

$$V = \rho j \quad (1)$$

where  $V$  is the potential gradient,  $\rho$  the resistivity, and  $j$  the current density vector. Except at a sink or a source, the current entering a volume of material has to equal the current leaving it i.e

$$\Delta \cdot j = 0 \quad (2)$$

From these two relationships can be calculated the potentials that can be expected, given boundary conditions (Keller and Frischknecht 1966, pp.90-196).

These two equations may be combined to obtain Laplace's equation:

$$-\Delta \cdot j = \frac{-1}{\rho} \Delta \cdot V = \frac{1}{\rho} \nabla^2 U = 0 \quad (3)$$

where  $U$  is a scalar potential function defined such that  $V$  is minus its gradient.

In cylindrical co-ordinates, whose origin is at  $P$  and whose  $z$  axis is vertical and positive downwards

$$\nabla^2 U = \frac{d^2 U}{dr^2} + \frac{1}{r} \frac{dU}{dr} + \frac{d^2 U}{dz^2} = 0 \quad (4)$$

with only a single current source, complete symmetry of current flow can be assumed, so derivatives taken in these directions may be eliminated, i.e.

$$\frac{d}{dr} \left( r^2 \frac{dU}{dr} \right) = 0 \quad (5)$$

Integrating

$$r^2 \frac{dU}{dr} = C$$

$$U = -\frac{C}{r} + D \quad (6)$$

When  $r$  is infinite,  $U$  is zero so the constant of integration  $D$  must be zero and  $C$  may be evaluated in terms of the current  $I$  from the source. Current density  $j$  should be uniform through the surface of a small sphere with radius  $A$  drawn around the current source. Total current  $I$  may be expressed as the integral of the current density over this surface.

$$\begin{aligned} I &= \int j \cdot ds \\ &= \int \frac{V}{\rho} ds \end{aligned} \quad (7)$$

$$\begin{aligned} I &= \int s \frac{C}{\rho r^2} ds \\ &= -\frac{2\pi C}{\rho} \end{aligned} \quad (8)$$

Solving for the constant of integration  $C$  and substituting

$$U = \frac{\rho I}{2\pi r} \quad (9)$$

The potential function is scalar, so that the potential at a point due to several sources can be added arithmetically.

$$U = \frac{\rho}{2\pi} \int_1^n \frac{I_n}{A_n} \quad (10)$$

Where  $I_n$  is the current from the  $n^{\text{th}}$  current electrode and  $A_n$  is the distance from the  $n^{\text{th}}$  source. Now in practice  $I$ , the current flowing and  $\Delta U$ , the potential between two points  $m$  and  $n$  are measured in the field.

So now

$$\rho = \left( \frac{U_m - U_n}{I} \right) \frac{2\pi}{\frac{1}{A_m} - \frac{1}{B_m} - \frac{1}{A_n} + \frac{1}{B_n}} \quad (11)$$

Where  $A_m$  and  $B_m$  are the distances of the current electrodes A and B from the measuring point m, likewise  $A_n$  and  $B_n$  are the distances of the current electrodes from point n.

This can be simplified to

$$\rho = \frac{\Delta U}{I} K \quad (12)$$

where K is the geometric factor depending on the electrode geometry,

The apparent resistivity of the anisotropic case can likewise be calculated (Keller and Frischknecht 1966, p.101) .

## 1.2 ELECTRICAL CONDUCTION IN ROCKS.

The method of conduction within rocks and minerals is complex and has been studied by many researchers. (Mining Geophysics Vol. II pp. 198-223).

"Conduction in most surface rocks, is largely electrolytic, taking place in the pore spaces and not significantly through the mineral grains. The ions which conduct the current result from the dissociation of salts, such dissociation occurring when salts are dissolved in water". (Ward and Fraser, 1967). It follows then, that the higher the ion concentration the lower the resistivity of the electrolyte.

Since the resistivity of the majority of minerals that make up the rock is usually well above that of the electrolyte, the resistivity of the rock depends on the porosity of the rock and the degree to which these pores are interconnected. The ratio of rock resistivity to electrolyte resistivity is the Formation factor (F) such that

$$F = \frac{\rho_r}{\rho_e}$$

where  $\rho_r$  is the saturated rock resistivity and  $\rho_e$  is the saturating electrolyte resistivity.

Some rocks do, however, contain minerals that conduct. Some of the most common of these are clay minerals, such as montmorillonite, illite, kaolinite and chlorite. Their bulk resistance is usually lower than their grain resistance because of a thick double layer of adsorbed cations. This double layer is due to unbalanced ion charges in the crystal lattice. These unbalanced charges are the result of broken bonds or aluminium substitutions in the silicon structure, aluminium being trivalent and silicon quadrivalent. The double layer consists of a fixed layer adjacent to the clay minerals and a diffuse layer whose ion concentration decreases exponentially with distance from the clay particle. This diffuse layer adds to the ion concentration and so decreases resistivity about the clay minerals.

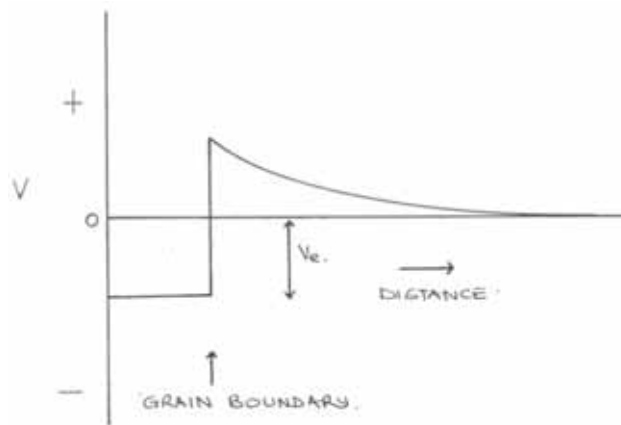
Of greater economic importance are the minerals in rocks that conduct electronically.

At an electrolyte-electronic conductor interface a potential barrier is set up which inhibits current flow. In the case of pyrite, Fe II ions tend to go into solution giving it an excess positive charge and leaving the pyrite grain with an excess negative charge.

The difference between the potential in the electronic conductor and the potential in the solution, at infinity, is the electrode potential,  $V_e$ . This potential varies with different minerals, and also depends upon the temperature and composition of the electrolyte. Fig. 1 shows the potential distribution about a sulphide grain in an electrolyte.

When a potential is applied across a grain the number of ions going into solution at one face increases while the number of ions going into solution at the other face decreases, thus the charge is transferred. In practice most ground water contains chloride ions, which on the application of a direct current form hydrochloric acid on one side of the grain. This causes oxidation - reduction reactions which affect the current flow by causing unbalanced potentials at each face. This means that an increased potential gradient is required to drive current from an electrolyte into an electronic conductor. This is referred to as over-voltage effect. (Keller and Frischknecht, 1966)

It can be seen that a current can be carried across an interface by two mechanisms. One involves the electrochemical reactions where an ion is converted to an atom, or an atom to an ion, and so the charge is physically



POTENTIAL DISTRIBUTION ABOUT A SULPHIDE  
IN AN ELECTROLYTE (Ward and Fraser, 1967)

### Figure 1 Potential distribution about a sulphide grain.

transported. The other mechanism involves charging and discharging the double layer around the mineral or clay grain, which forms a capacitive coupling through the electrolyte. Neither mechanism is purely resistive and the resistance varies roughly, with the inverse of the square root of the frequency. This impedance is known as the Warburg impedance (Warburg, 1899, 1901).

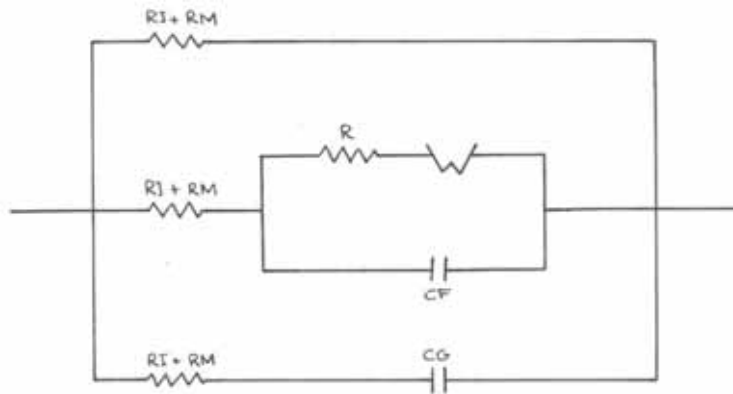
Above 1000 Hz most of the current is carried across the interface by capacitive coupling, while at lower frequencies a resistive path predominates, but still in series with the Warburg impedance. Many analog models have been designed to represent this conduction. (Ward and Fraser, 1967, pp. 209). Fig. 2 is such a model.

In Figure 2.

- RI - Resistance of ionic path
- RM := Resistance of metallic grain
- R = Reactance resistance
- CF = Double layer capacitance
- W = Warburg impedance

Where clay minerals make up more than 10% of the rock, membrane polarization has an appreciable effect on the electrical conduction

(Ward and Fraser, 1967). The cations that accumulate around the clay mineral slow or



EQUIVALENT CIRCUIT REPRESENTING MASSIVE AND DISSEMINATED MINERALISED ROCKS

**Figure 2 IP Equivalent Circuit.**

stop the flow of negative ions through the system when a current is applied. This causes a voltage gradient which opposes the flow of current. At higher frequencies, about 1000 Hz, this voltage gradient becomes insignificant because the mobility of the ions is not reduced. Because of the above phenomenon the voltage and current are not usually in phase. Hence we may write Ohm's law as

$$j = \{ \sigma (\omega) - i \omega \sigma p(\omega) \} V$$

where j is the current through the rock, V is the voltage across the rock,  $\omega$  is the angular frequency,  $\sigma(\omega)$  the conductance and  $\sigma p(\omega)$  the equivalent dielectric constant.

If electromagnetic methods are used even greater control and information is achieved. The telluric resistivity method uses natural A.C. fields flowing within the earth and allows the measurement of relative resistivities between locations, while the magnetotelluric method gives absolute resistivities.

Controlling the source of the electromagnetic waves gives greater flexibility in interpretation. Various methods have been developed using time varying magnetic fields generated by an alternating current in a loop of wire, or a grounded wire. Conductors present within the ground produce secondary fields which distort the primary field. Maxwell's equations can be used to describe the currents and fields within the conductive medium.

All these methods are able to evaluate resistivity or resistivity contrasts. They do not discriminate between different types of conductors.

### **1.3 NON-LINEAR CONDUCTION.**

The conduction in most homogeneous materials is linear, that is the current-voltage graph is a straight line. This relationship holds also for semiconducting materials. But in reality there is always some heterogeneity. In the more usual case of multi-mineral aggregates the inhomogeneity is quite complex. It is this inhomogeneity that causes non-linear conduction within semi-conductors.

Table 1 contains a list of some semi-conducting minerals and their resistivities (Keller and Frischknecht, 1966, pp 5-6). The large range of resistivities is in part due to the fact that many of the minerals listed have an indefinite composition and the electrical properties may be altered considerably by minor changes in composition. The reason for this is explained in Chapter 2.

Conduction in the ground, especially in non-mineralized areas, is principally through fluid electrolytes that saturate the rocks. There are a few exceptions, however, one of the main ones being carbon in black graphitic shales. In most surveys done in the search of ore bodies carbon behaves in the same manner as sulphides and great difficulty is experienced in separating the effects of these different conductors.

TABLE 1

Resistivities of semiconducting minerals (zero frequency)

<u>Native elements</u>	
Diamond (C)	2.7 ohm-m
<u>Sulphides</u>	
Argentite, $Ag_2S$	$1.5$ to $2.0 \times 10^{-3}$
Bismuthinite, $Bi_2S_3$	3 to 570
Bornite, $Fe_2S_3 \cdot nCu_2S$	$1.6$ to $6000 \times 10^{-6}$
Chalcocite, $Cu_2S$	$80$ to $100 \times 10^{-6}$
Chalcopyrite, $Fe_2S_3 \cdot Cu_2S$	$150$ to $9000 \times 10^{-6}$
Covellite, $CuS$	$0.30$ to $83 \times 10^{-6}$
Galena, $PbS$	$6.8 \times 10^{-6}$ to $9.0 \times 10^{-2}$
Haverite, $MnS_2$	10 to 20
Marcasite, $FeS_2$	$1$ to $150 \times 10^{-3}$
Metacinnabarite, $4HgS$	$2 \times 10^{-6}$ to $1 \times 10^{-3}$
Millerite, $NiS$	$2$ to $4 \times 10^{-7}$
Molybdenite, $MoS_2$	0.12 to 7.5
Pentlandite $(Fe, Ni)_9S_8$	$1$ to $11 \times 10^{-6}$
Pyrrhotite, $Fe_7S_8$	$2$ to $160 \times 10^{-6}$
Pyrite, $FeS_2$	$1.2$ to $600 \times 10^{-3}$
Sphalerite, $ZnS$	$2.7 \times 10^{-3}$ to $1.2 \times 10^4$
<u>Antimony - sulfur compounds</u>	
Berthierite, $FeSb_2S_4$	0.0083 to 2.0
Boulangerite, $Pb_5Sb_4S_{11}$	$2 \times 10^3$ to $4 \times 10^4$
Cylindrite, $Pb_3Sn_4Sb_2S_{14}$	2.5 to 60
Franckeite, $Pb_5Sn_3Sb_2S_{14}$	1.2 to 4
Hauchecornite, $Ni_9(Bi, Sb)_2S_8$	$1$ to $83 \times 10^{-6}$
Jamesonite, $Pb_4FeSb_6S_{14}$	0.020 to 0.15
Tetrahedrite, $Cu_3SbS_3$	0.30 to 30,000
<u>Arsenic-sulfur compounds</u>	
Arsenopyrite, $FeAsS$	$20$ to $300 \times 10^{-6}$
Cobalite, $CoAsS$	$6.5$ to $130 \times 10^{-3}$
Enargite, $Cu_3AsS_4$	$0.2$ to $40 \times 10^{-3}$
Gersdorffite, $NiAsS$	$1$ to $160 \times 10^{-6}$
Glaucodote $(Co, Fe)AsS$	$5$ to $100 \times 10^{-6}$

TABLE 1 (cont.)

Antimonide

Dyscrasite,  $\text{Ag}_3\text{Sb}$  0.12 to  $1.2 \times 10^{-6}$

Arsenides

Allemonite,  $\text{SbAs}_3$  70 to 60,000  
 Lollingite,  $\text{FeAs}_2$  2 to  $270 \times 10^{-6}$   
 Nicollite,  $\text{NiAs}$  0.1 to  $2 \times 10^{-6}$   
 Skutterudite,  $\text{CoAs}_3$  1 to  $400 \times 10^{-6}$   
 Smaltite,  $\text{CoAs}_2$  1 to  $12 \times 10^{-6}$

Tellurides

Altaite,  $\text{PbTe}$  20 to  $200 \times 10^{-6}$   
 Calavarite,  $\text{AuTe}_2$  6 to  $1\text{w} \times 10^{-6}$   
 Coloradoite,  $\text{HgTe}$  4 to  $100 \times 10^{-6}$   
 Hessite,  $\text{Ag}_2\text{Te}$  4 to  $100 \times 10^{-6}$   
 Nagyagite,  $\text{Pb}_6\text{Au}(\text{S},\text{Te})_{14}$  20 to  $80 \times 10^{-6}$   
 Sylvanite,  $\text{AgAuTe}_4$  4 to  $20 \times 10^{-6}$

Oxides

Braunite,  $\text{Mn}_2\text{O}_3$  0.16 to 1.0  
 Cassiterite,  $\text{SnO}_2$   $4.5 \times 10^{-4}$  to 10,000  
 Cuprite,  $\text{Cu}_2\text{O}$  10 to 50  
 Hollandite,  $(\text{Ba},\text{Na},\text{K})\text{Mn}_8\text{O}_{16}$  2 to  $100 \times 10^{-3}$   
 Ilmenite,  $\text{FeTiO}_3$  0.001 to 4  
 Magnetite,  $\text{Fe}_3\text{O}_4$   $52 \times 10^{-6}$   
 Manganite,  $\text{MnO.OH}$  0.018 to 0.5  
 Melaconite,  $\text{CuO}$  6000  
 Psilomelane,  $\text{KMnO.MnO}_2.n\text{H}_2\text{O}$  0.04 to 6000  
 Pyrolusite,  $\text{MnO}_2$  0.007 to 30  
 Rutile,  $\text{TiO}_2$  29 to 910  
 Uraninite,  $\text{UO}$  1.5 to 200

Keller and Frischknecht (1966) p.5.

One possible method of differentiating the two could be in the study of the linearity of electrical conduction in rocks containing sulphide and shales. The feasibility of this method is examined in this thesis.

It was decided to approach the problem by studying conduction through cores of natural rock in the laboratory.

Cores containing semiconducting minerals would be more likely to show nonlinear effects, with current density, than cores containing only metallic type conducting minerals such as graphite. Table 2 contains the resistivities of some metals and metallic minerals. An account of the processes of semiconduction is presented in Chapter 2.

Another possible source of nonlinear conduction could occur at a fluid electrolyte-solid interface within the rock. The nonlinearity of conduction at this interface may be due to electrochemical reaction, and subsequent formation of oxidation-reduction products on the interface. Electrolyte-solid interfaces have been investigated by other researchers (Madden, 1961) and are not dealt with in this thesis.

TABLE 2

Resistivities of metals and metallic minerals (zero frequency)

<u>Refined metals at 0°C</u>	
Lithium	$8.5 \times 10^{-8}$ ohm-m
Beryllium	$5.5 \times 10^{-8}$
Sodium	$4.3 \times 10^{-8}$
Magnesium	$4.0 \times 10^{-8}$
Aluminium	$2.5 \times 10^{-8}$
Potassium	$6.3 \times 10^{-8}$
Calcium	$4.2 \times 10^{-8}$
Titanium	$83 \times 10^{-8}$
Chromium	$15.3 \times 10^{-8}$
Iron	$9.0 \times 10^{-8}$
Cobalt	$6.3 \times 10^{-8}$
Nickel	$6.3 \times 10^{-8}$
Copper	$1.6 \times 10^{-8}$
Zinc	$5.5 \times 10^{-8}$
Gallium	$41 \times 10^{-8}$
Arsenic	$35 \times 10^{-8}$
Rubidium	$11.6 \times 10^{-8}$
Strontium	$33 \times 10^{-8}$
Zirconium	$42 \times 10^{-8}$
Molybdenum	$4.3 \times 10^{-8}$
Ruthenium	$11.7 \times 10^{-8}$
Rhenium	$4.5 \times 10^{-8}$
Palladium	$10.0 \times 10^{-8}$
Silver	$1.5 \times 10^{-8}$
Cadmium	$6.7 \times 10^{-8}$
Indium	$8.5 \times 10^{-8}$
Tin	$10.0 \times 10^{-8}$
Antimony	$36 \times 10^{-8}$
Cesium	$18 \times 10^{-8}$
Barium	$59 \times 10^{-8}$
Lanthanum	$59 \times 10^{-8}$

TABLE 2 (cont.)

Cerium	$71 \times 10^{-8}$
Praseodymium	$62 \times 10^{-8}$
Hafnium	$29 \times 10^{-8}$
Tantalum	$14 \times 10^{-8}$
Tungsten	$5.0 \times 10^{-8}$
Osmium	$9.1 \times 10^{-8}$
Iridium	$5.0 \times 10^{-8}$
Platinum	$9.8 \times 10^{-8}$
Gold	$2.0 \times 10^{-8}$
Tellurium	$14 \times 10^{-8}$
Lead	$19 \times 10^{-8}$
Bismuth	$100 \times 10^{-8}$

Metallic minerals

Native copper	$1.2 \text{ to } 30 \times 10^{-8} \text{ ohm-m}$
Graphite (carbon)	$36 \text{ to } 100 \times 10^{-8}$ (current flow parallel to cleavage)
	$28 \times 9900 \times 10^{-6}$ (current flow across cleavage)
Ulmanite, NiSbS	$9.0 \text{ to } 120 \times 10^{-8}$
Breithauptite, NiSb	$3.0 \text{ to } 50 \times 10^{-8}$

Keller and Frischknecht (1966) p.4.

## 1.4 PREVIOUS WORK.

Published work on nonlinear conduction in minerals is limited to two main sources, one Russian and one Canadian. The Russian work was mainly produced by Y.B. Shaub and is reported in a series of papers published in the Bulletin of the Academy of Sciences, Earth Physics. His first (Shaub, 1965) discussed some of the theoretical aspects of nonlinear conduction in rocks, as a tool for electrical prospecting. The use of a two frequency method was discussed, along with possible methods of analysis. He proposed five types of nonlinear conduction:

- a. proportional to current strength.
- b. proportional to the modulus of current strength.
- c. proportional to the square of current strength.
- d. proportional to the cube of current strength .
- e. dependent not on the strength but only on the direction of the current.

He also stated that "these effects, or at least some of them, decrease as frequency rises".

In a paper in the same publication (Shaub, 1969) he developed his ideas further and looked at the possibility of detecting a conductive spherical body. He also showed a plot of current density versus signal amplitude at the mixing frequency for five substances; brass, chalcopyrite, pyrrhotite, graphite and galena. Comparison of his results is difficult since it is not clear what he plotted for his signal amplitude.

His third paper (Shaub, 1971(a)) showed the results he achieved using a model bore hole. A bore hole was used in order to achieve high current densities ( $> 20 \text{ mA/Cm}^2$ ). He observed a certain amount of non-repeatability of results (approximately 12%) and attributed this to changes within the model and on its surface, caused by high current

densities.

Shaub's next two papers were also published in 1971 (Shaub 1971(b), and 1971 (c)). The first was a model study done in an electrolytic tank using zinc, copper and lead sheets as conductors. In this work he does not seem to have considered what mechanisms were causing the effects. He noted that these effects were only present after the sheets had been left in the electrolyte for a period of time, being several times larger after a period of about ten days in the tank.

The second paper refers to work done on actual bore holes in the area of the Kimovsk deposit. He showed that it was possible to differentiate between various zones of mineralization but gave no indication of what these zones were, excepting one which contained mainly galena.

Shaub, in most of his work, made no reference to the origins of the nonlinear effects, nor did he consider that they may have come from his own electrodes. He did, in one paper, prove that the electrode used could have caused the effect he was measuring but made no reference to this in field studies.

Research done by the Canadian Geological Survey into nonlinear electrical phenomena was reported in a paper by Katsube, Ahrens and Collett (1973). In their work they use what is basically a single frequency method, studying the distortion in Lissajous figures caused by nonlinear conduction. When using frequencies below 1 Hz they incorporated a 1 kHz modulator which helped in amplification problems. They also studied phase relationships of the modulator as the carrier signal varied.

In this paper they suggested that electrical nonlinear phenomena occur above a certain charge density. This critical charge density is dependent on frequency in such a way that the charge density necessary to achieve nonlinearity decreases with decreasing frequency. Nonlinear effects were noted in a serpentinite sample and it was suggested the nonlinear conduction occurred at microfractures

within the sample. They also tested a galena sample and concluded that the effects took place at the electrolyte-mineral interface. They also suggested that charge densities necessary to achieve nonlinear conduction could only be achieved in bore holes.

## 2. SEMI-CONDUCTION

### 2.1 THE MECHANISM OF CONDUCTION IN SEMI-CONDUCTORS.

The conduction of electricity in semi-conductors is similar to the conduction in metals, in that it is by electron motion. Metals have "cloud of free electrons" so conduction is high. Semi-conductors have a higher resistivity than metals but this is not due to lower electron mobility but is due to fewer free electrons. This means that the energy level of the conduction electrons must be raised before these electrons are freed to take part in conduction. This energy is in the form of heat so that these materials exhibit a negative temperature coefficient of the resistivity, at least over part of the temperature range. Fig. 3 shows two typical cases encountered in practice.

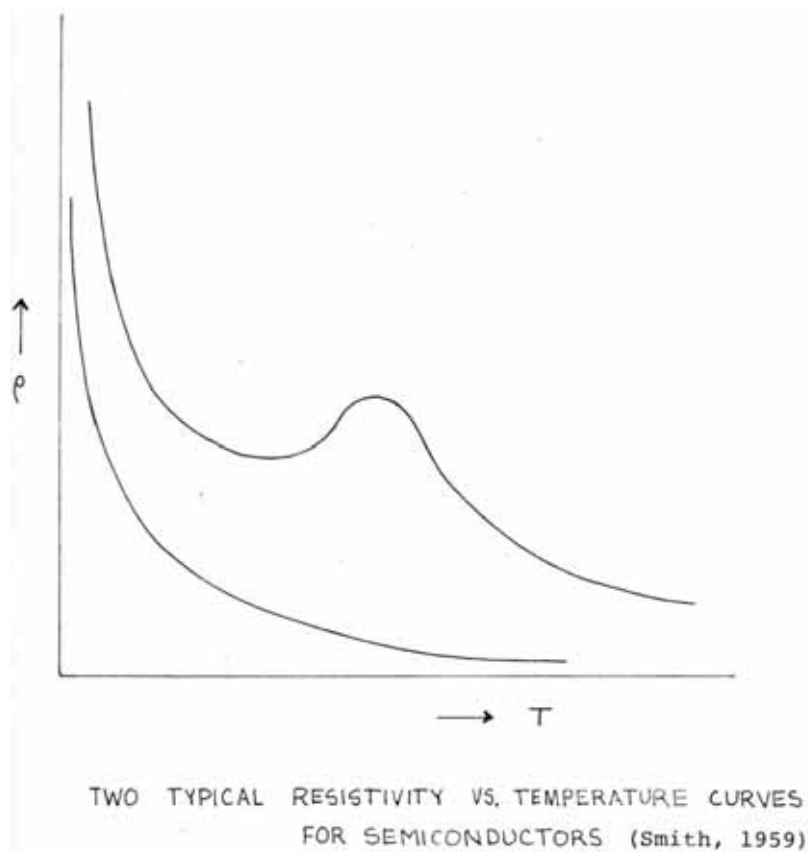


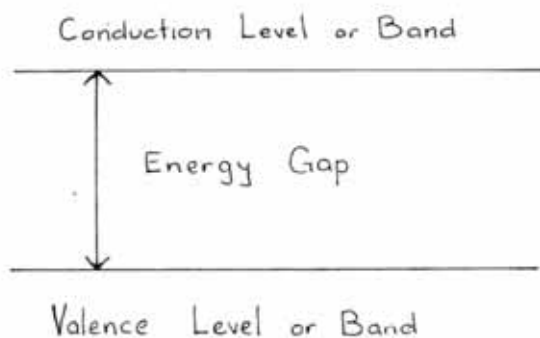
**Figure 3 Resistivity vs Temperature for Semiconductors.**

This negative  $d\rho/dT$  is a generally accepted basis for classifying a material as a semi-conductor. Insulators also have a negative  $d\rho/dT$  and in this respect behave as semi-conductors. Semi-conductors and insulators differ only in the magnitudes of their resistivity.

Looking more closely at the crystal lattice of semiconductors we see that at absolute zero temperature, all the electrons are bonded and are not free to move through the crystal. Thus at absolute zero all semiconductors are insulators, unlike metals which always have 'free' electrons. As the temperature rises some of the valence electrons may absorb enough energy from lattice vibration to be released from the bonds, and so move through the crystal and contribute to the conductivity. It should be noted that the electron when it breaks a bond leaves a 'hole' which moves in the same direction as the positive charge carrier.

For a pure element such as Ge and Si the number of free electrons must equal the number of mobile holes. These types of semiconductors are called intrinsic semiconductors and must be distinguished from extrinsic semiconductors in which the charge carriers (electrons or holes) are present as a result of impurities built into the crystal.

As was seen, at absolute zero all valence electrons in a semiconductor take part in the bonds between the atoms. Also these electrons may become free after the absorption of a sufficient amount of energy, that is, free electrons have a greater amount of energy than bonded ones.



SCHMATIC DIAGRAM SHOWING ELECTRON LEVELS

**Figure 4. Schematic Diagram showing Electron Levels.**

Referring to Fig. 4 we see the electrons have two states, one at the valence level and one at the conduction level. They have to absorb enough energy to get over this energy gap. In practice all valence electrons do not have the same energy, nor do the conduction electrons have the same energy but rather they have energy bands.

In the case of extrinsic semi-conductors the impurities (or doping compounds) make available extra electrons which occupy states or energy levels within the energy gap. These states are known as donor levels and electrons in these levels do not have to absorb as much energy to jump into the conduction band. This effectively lowers the resistivity of the crystal.

This doping provides extra electrons or holes depending on the impurities present. If the material has an 'excess' of electrons it is called n-type, if it has an 'excess' of holes it is called p-type.

When p-type and n-type material are brought together a p-n junction is formed. The n-type material has an excess of electrons while the p-type contains an excess of holes, so when they are brought into contact the electrons diffuse into the p material and the holes diffuse into the n material. This sets up a potential gradient across the junction called the contact potential. Electrons going from the n to the p material must go up This potential hill. If this junction is biased so as to make the n-region negative with respect to the p-region the potential difference or hill between the material is lowered so the current or electrons will flow more easily across the junction. The probability that an electron will climb the hill is increased by a factor of  $e^{eV/kT}$  where V is the applied potential between the p and n region. Consequently for the biased junction there will be a net electron current given by

$$J_e = J_{e0} (e^{eV/kT} - 1) \quad (15)$$

Where k is Boltzmann's factor and T is temperature, e is electronic charge and  $J_{e0}$  is the net current density of electrons.

The biased junction carries a net hole current

$$J_h = J_{h0} (e^{eV/kT} - 1) \quad (16)$$

where  $J_{ho}$  is the net charge density of holes.

The total current is given by the sum of (15) and (16)

$$J = (J_{eo} + J_{ho}) (e^{eV/kT} - 1) \quad (17)$$

Since  $(J_{eo} + J_{ho})$  is a constant, the current density increases exponentially with the voltage when applied so as to make the n-region negative with respect to the p-region. This is called a forward bias.

For the reversed biased situation

$$J = (J_{eo} + J_{ho}) (1 - e^{-eV/kT}) \quad (18)$$

The reverse current approaches saturation as the reverse bias is increased. It is observed that this junction has a non-linear current-voltage characteristic Fig. 31. A more quantitative treatment of p-n junctions is given in Chapter 4.

## 2.2 SEMI-CONDUCTING MINERALS.

The first feature used to distinguish semi-conductors was their negative temperature coefficients of resistance. This was first done by Michael Faraday in work involving silver sulphide. In 1873 F. Braun discovered the phenomenon of rectification using substances like lead sulphide and iron pyrites. The discovery of the "Hall effect" in 1879 made it possible to distinguish semi-conductors from other poorly conducting substances. This led to a lot of systematic work being done on the properties of semi-conductors. During some of this work rectification was identified as a surface effect. The first important application of semi-conductors was to provide rectifiers for low frequency A.C. currents (1886). In 1904 Bose patented a rectifying device for higher frequencies. A fine wire or 'cats whisker' in contact with a crystal of semi-conducting material made an excellent rectifier. The materials generally preferred were silicon and lead sulphide (galena). Since this time most of the work has been with silicon and germanium. Recently, though, sulphides have come under increased scrutiny. A coverage of semi-conductor physics can be found in a book by Smith (1959).

Lead is probably the sulphide about which most is known. It has a small forbidden energy gap of about 0.3 eV, and moderate value of electron and hole mobilities. It can also exist as p and n-type material depending on impurities. The properties depend very much on the surface properties of the individual grains and on the form of contact between them.

Little at present is known about energy levels associated with impurities in lead sulphide. The addition of various impurities is known to give rise to donor or acceptor levels; Bi acts as a trivalent ion and so behaves as a donor, while Ag and Cu behave as monovalent ions and act as acceptors, each replacing a  $\text{Pb}^{2+}$  ion.

Also  $\text{Cl}^-$  replaces a  $\text{S}^{2-}$  ion acting as a donor. An excess of lead in lead sulphide produces donor levels, while excess S produces acceptor levels. If crystals of lead sulphide are brought into equilibrium with sulphur vapour and then cooled rapidly, it is found that the carrier concentration is a function of the partial pressure of the sulphur vapour.

For high pressures of sulphur vapour ( $P_s$ ), p-type conduction is found, and for low values of  $P_s$  the conduction is n-type. For any given temperature at which the equilibrium is established there is a critical value of  $P_s$  for which a change from n-type to p-type takes place. Adding impurities such as Cu, Ag and Bi changes the partial pressure of S needed to produce near-intrinsic material.

Other sulphides have been studied to a far lesser extent and very little is known about them.  $Cu Fe S_2$  has been studied and shows rectification at a metal point contact. It has a forbidden energy gap of about 0.5 eV. Compounds like  $Cu_2 Fe Sn S_4$  should also show semi-conducting properties.

Many oxides show semi-conducting properties.  $Cu_2O$  was studied because of its early use in rectifiers. Normally  $Cu_2O$  is a p-type semiconductor with a forbidden energy gap between 1.5 and 1.9 eV depending on the way it was measured. It appears impossible to get n-type  $Cu_2O$  even with low  $O_2$  partial pressures.  $ZnO$  has a higher forbidden energy gap, 3.2 eV, mainly due to excess Zn, which means that the crystals are n-type.  $TiO_2$  behaves in much the same manner being n-type with about 3 eV energy gap. These oxides have a high resistivity.

Nickel and iron oxides have generally a low resistivity, down to about  $10^{-2}$  ohm-m. This is mainly due to the fact that the metal ion has variable valency. For example Fe can readily occur as  $Fe^{2+}$  and  $Fe^{3+}$  in certain crystals such as magnetite ( $Fe_3O_4$ ). This can be rewritten  $(2Fe^{3+} + Fe^{2+})O_4^{2-}$  the extra electron on  $Fe^{2+}$  can jump to  $Fe^{3+}$  and so can move through the crystal. Similarly Ni can exist as  $Ni^{2+}$  and  $Ni^{3+}$  and the addition of a small monovalent impurity will lower the resistivity. The conductivity in these oxides is P-type (Smith, 1959).

It can easily be seen that the conductivity in ore deposits is going to be extremely complex, with many different minerals present containing different and unknown impurity levels. Some of these properties are going to depend on current densities while others will depend on voltage gradients across interfaces and grain boundaries.



### 3. EXPERIMENTAL METHODS AND RESULTS

#### 3.1 CURRENT DENSITIES.

Most of the early laboratory work done on the conduction of electricity in rocks was done using high current densities, typically of the order of 10mA/cm<sup>2</sup>. Anderson and Keller (1964) in a study of induced polarization noted that "laboratory studies of induced polarization, in which high current densities were used, may provide highly misleading results". They point out that "laboratory measurements of polarization will show values that" are much lower than those obtained in the field" (because of differences in current densities).

The current densities in a homogeneous half space can easily be calculated using equation (19).

$$J = \frac{I}{2\pi R_1^2} - \frac{I}{2\pi R_2^2} \quad (19)$$

Where J is the current density, I is the input current, and R<sub>1</sub> and R<sub>2</sub> are the distance from the current electrodes to the point of measurement.

Table 3 gives the current densities in μA/cm<sup>2</sup> at various distances from an electrode I<sub>1</sub> (I<sub>2</sub> at infinity).

DISTANCE (m)	CURRENT DENSITIES ( $\mu\text{A}/\text{cm}^2$ )
4	1
10	.16
40	.01
100	.0016

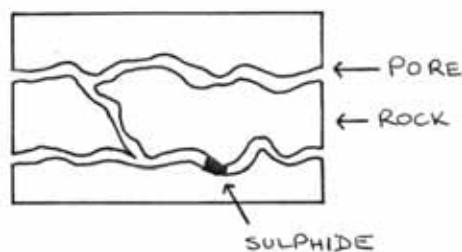
TABLE 3.

CURRENT DENSITIES AT DISTANCES  
FROM AN ELECTRODE WITH 1 AMP  
INPUT

From Table 3 it can be seen that current densities used in the laboratory have to be  $1\mu\text{A}/\text{cm}^2$  or lower for the results to be of use when comparing field situations. To calculate the actual current density across one grain of sulphide in a rock can prove difficult.

The conduction in rocks is mainly through electrolytes filling inter-connecting pore spaces rather than through the whole rock.

If the model of Fig. 5 had a cross-sectional area of  $1\text{ cm}^2$  and  $1\mu\text{A}$  was passed through it, the resultant current density across the sulphide grains would be considerably higher than  $1\mu\text{A}/\text{cm}^2$  since the actual path of conduction is essentially restricted to the electrolyte path. This could raise the current densities across a sulphide grain to tens of  $\mu\text{A}/\text{cm}^2$ .

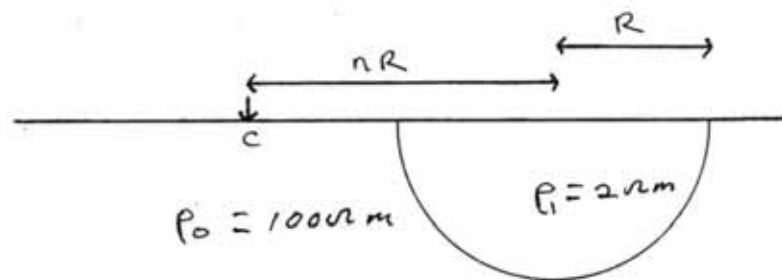


SIMPLIFIED CONDUCTION PATH IN MINERALIZED ROCK

**Figure 5 Simplified Conduction Path in Mineralised Rock.**

Most sulphide ore bodies are more conductive than their surrounding host rock. In a homogeneous half-space with an ore body, say 10 times as conductive as its host, the body will tend to distort the current flow so that more current will flow through it. This means that current densities across sulphide grains at the boundaries of the ore body, and within the pores or cracks, will be slightly higher than expected.

It can be shown that the current flowing through a body, as in Fig 6, is over twice as great as that flowing across the homogeneous half space without the body if  $\rho_0 = 100 \Omega^{-m}$  and  $\rho_1 = 2 \Omega^{-m}$  and the current electrode is at a distance of 20 times the radius of the body. If  $\rho_0 = 100 \Omega^{-m}$  and  $\rho_1 = 2 \Omega^{-m}$  and the current electrode is at a distance of 8 times the radius of the body then the ratio of current flowing with and without the body is 250.



MODEL USED IN CURRENT DENSITY CALCULATIONS

**Figure 6 Model used for current density calculations.**

This may mean that current densities across sulphide electrolyte interfaces in the ground may be as high as several hundred microamps per square centimetre.

### 3.2 SINGLE FREQUENCY METHOD OF MEASURING NON-LINEAR CONDUCTION.

When a sinusoidal voltage is applied to a linear network, the current that flows is non-distorted (i.e. sinusoidal) but may lag or lead the applied voltage. If there is a non-linear element present then the current waveform may become distorted. In the simplest linear system a plot of current against voltage yields a straight line whose slope depends on resistance. If a non-linear element is present then the plot becomes distorted as in Fig.7

Providing. the resistance of the sample is reasonably high, compared to the generator's output impedance, then the voltage that is applied remains linear as the current is distorted. If the network only contains a small non-linear element then the current will contain a large linear element. The non-linear portion of the curve (Fig. 7) is of main interest so that if the linear segment is removed the residue can be amplified.

In practice the linear element can simply be removed by the use of a bridge circuit. When balanced for any one voltage it will give a zero reading but as the voltage is changed any non-linear element present will disturb this balance and should give a curve of the form seen in Fig 8.

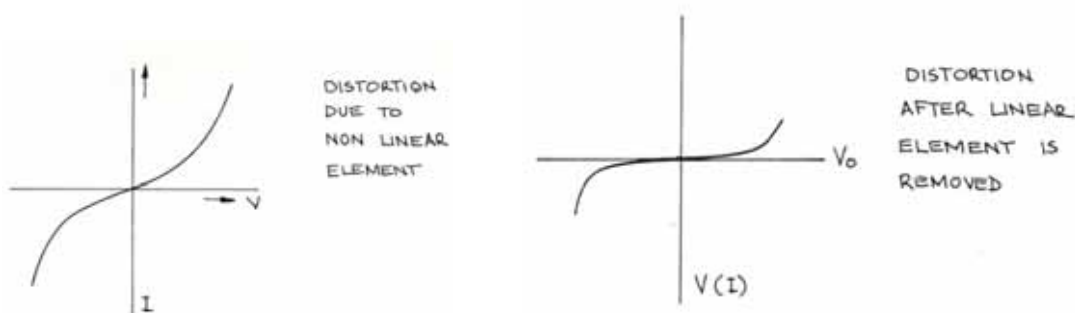


**Figure 7 Distortion due to non linear element.**

**Figure 8 Distortion after removal of linear element.**

The voltage across the bridge, (Fig. 9) can be calculated in terms of change in resistance of the rock sample, the resistance of the rock here being  $R_1 + \Delta R$ .

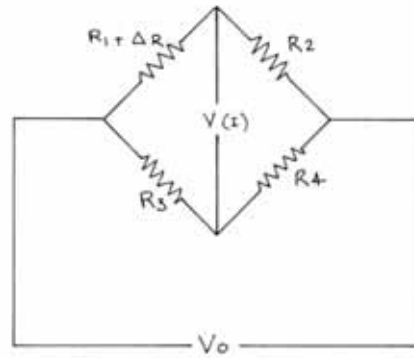
Where  $R_2$ ,  $R_3$  and  $R_4$  are balancing resistors,  $V(I)$  is the unbalanced voltage across the bridge and  $V_A$  is the voltage activating the bridge.  $\Delta R$  is the non-linear resistance of the rock.

At balance  $V(I) = 0$

$$\frac{R_1}{R_2} = \frac{R_3}{R_4} \quad (20)$$

and off balance

$$\begin{aligned} V(I) &= V_0 \left[ \frac{R_1 + \Delta R}{R_1 + \Delta R + R_2} - \frac{R_1}{R_1 + R_2} \right] \\ &= V_0 \left[ \frac{(R_1 + \Delta R)(R_1 + R_2) - R_1(R_1 + \Delta R + R_2)}{(R_1 + \Delta R + R_2)(R_1 + R_2)} \right] \\ V(I) &= V_0 \frac{R_1^2 + R_1 R_2 + \Delta R R_1 + \Delta R R_2 - R_1^2 - \Delta R R_1 - R_1 R_2}{(R_1 + R_2)^2 \left[ 1 + \frac{\Delta R}{R_1 + R_2} \right]} \\ &= V_0 \frac{\Delta R \cdot R_2}{(R_1 + R_2)^2 \left( 1 + \frac{\Delta R}{R_1 + R_2} \right)} \quad (21) \end{aligned}$$



BRIDGE USED TO  
REMOVE LINEAR  
ELEMENT

**Figure 9 IP Bridge used to remove linear element.**

This can be used to evaluate the linearity of the cores.

$$V(I) \approx V_0 \frac{\Delta R R_2}{(R_1 + R_2)^2} \quad (22)$$

If  $R_1 = R_2$

$$V(I) \approx V_0 \frac{\Delta R}{4R_1} \quad (23)$$

$$\frac{V(I)}{V_0} = \frac{\Delta R R_2}{(R_1 + R_2)^2} \quad (24)$$

If  $R_2 \gg R_1$

$$\frac{V(I)}{V_0} \approx \frac{\Delta R}{R_2} \quad (25)$$

### 3.3 METHOD OF MEASUREMENT.

Some time has been spent in looking at the best type of sample electrodes. The electrodes have to be able to pass a current through the rock specimen without affecting the rock or causing non-linear effects at the electrode contacts.

A copper-copper sulphate cell was tested but found to be unsuitable because the noise level was high, and also because of the uncertainty of behaviour of the  $\text{CuSO}_4$  on the rock interface. When studying dry rock cores this method becomes unsuitable.

Another system tried consisted of metallic copper electrodes clamped to each end of the core. This gave noisy and unrepeatable results. Although some sign of non-linearity was present, this could have been due to the point contacts made between the sulphides on the end of the core and the copper electrodes. To overcome this, the ends of the cores were painted with silver dag, which gave less noisy results and better contacts. However, the method was discarded because the silver reacted with the sulphide present to give silver sulphide. Gold plating the contact areas was considered but not used. Copper gauze compressed behind filter paper was also tested, but again proved noisy.

The best method found is a cell using powdered graphite electrodes. This consists of a copper plate mounted on 1 cm Perspex. The graphite forms a conducting layer between the copper and the core. The cell is illustrated in Fig. 10.

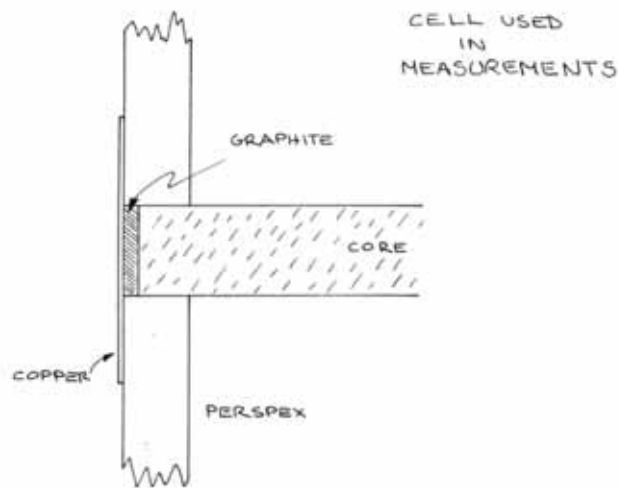


**Figure 10 Cell used in Measurements.**

Skov and Pearlstein (1965) tested various electrodes while studying non-linear ionic conductivity in electrode materials: graphite, gold, copper, silver, nickel and aluminium. All these electrodes proved to be linear, except aluminium and copper, if their surfaces were allowed to deteriorate. If the aluminium and copper electrodes had clean surfaces they conducted linearly. As was noted earlier, Shaub (1971 (b)) observed the same effects but he also failed to give an explanation for the non-linearity. The explanation probably lies in the fact that contacts such as copper-copper oxide are non-ohmic and the electrodes involved form oxides on their surfaces thus forming non-linear contacts.

Care has to be taken in packing the graphite to get even coverage otherwise non-linearities will occur due to high current densities passing through small areas.

Graphite is linear at the current densities used but at high values tends to conduct non-linearly.

The graphite provides a good even contact to the cores while not affecting them chemically. Graphite allows the testing of wet or dry cores. The cell was tested using a brass core which gave a linear response over a large range of currents, up to 3 orders of magnitude above those needed (10mA).

This cell is used in one arm of a wheatstone bridge which is used to remove the linear component of the current. The circuit used is shown in Fig. 11.

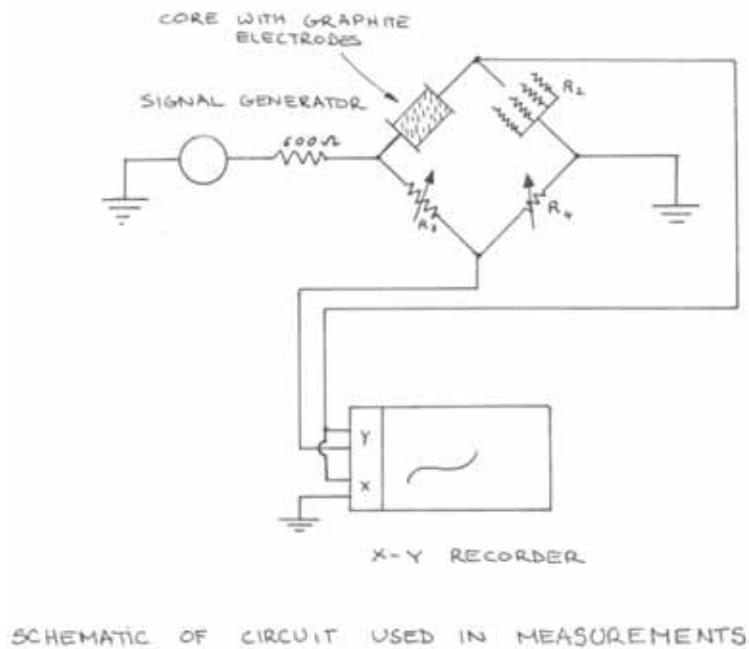


**Figure 11. Schematic of Circuit used in Measurements.**

The bridge excitation was supplied by a signal generator (I.E.C. Type Model T.W.G. 501) which can operate in the frequency range 0.001 Hz to 1 MHz at output voltages from 0 to 20 volts peak to peak. The generator output was connected to the circuit through a 500Ω resistor to ensure that the bridge impedance was greater than the generator's output impedance (500Ω).

The output of the bridge was fed into the y axis amplifier of an x-y recorder (Rikadenki, model BW10) while the x axis amplifier was fed with the voltage that was dropped across the resistor in the upper right hand side of the bridge in Fig. 11. This produced a plot of distortion versus current density.

All samples used for testing were cores, most of which were 2.25 cm. diameter. Some were 2.05 cm. diameter. The length varied from 3 cm. to 8 cm.

The cores were first dried in an electric oven for 1 hour at 110°C. They were then placed in a vacuum flask, evacuated and left evacuated for 24 hours. The electrolyte was introduced into the flask and the rocks left soaking for at least 24 hours before being placed in the measuring cell.

To ensure that the conduction did not take place along the surface of the core it was left to dry for several minutes, before being wrapped in insulating tape, to restrict further drying.

After testing, the samples were washed in an ultrasonic cleaner to remove the graphite electrodes and then re-dried. When the cores were again re-saturated they had the same resistivity as previously ( $\pm 5\%$ ).

### 3.4 RESULTS.

Several cores were tested including sandstone, massive sulphides and disseminated sulphides. (See CH 3.7)

The sandstone remained linear from low currents up into the milliamp range. This gave a good indication that there were no non-linear elements inherent in the system. When the sandstone was tested dry its resistance was well over 200 M $\Omega$ .

A massive sulphide was also tested. This core consisted almost entirely of fine grained pyrite with very minor chalcopyrite present. The resistance of this core was 0.5 $\Omega$ . Because of its low resistance problems were encountered in achieving low current densities. To achieve low currents very low voltages had to be used. This created a noise problem but even so no or only very slight non-linearity was indicated.

A disseminated sulphide of sphalerite and pyrite was also tested. The sulphide made up about 50% of the core with a slight predominance of pyrite over the sphalerite. Very minor chalcopyrite was also present.

The dried core was tested with two voltages across the bridge, one being 4 - 5 V r.m.s., the other 0.49 V r.m.s. At low current a small amount of non-linearity could be seen along with considerable noise. The sample was tested using three different frequencies. (0.1Hz, 0.03Hz, and 0.01Hz). The results can be seen in Fig. 12.

It is difficult to put a zero voltage line on these curves due to the drift that is present. This drift causes the zero voltage line to be curved.

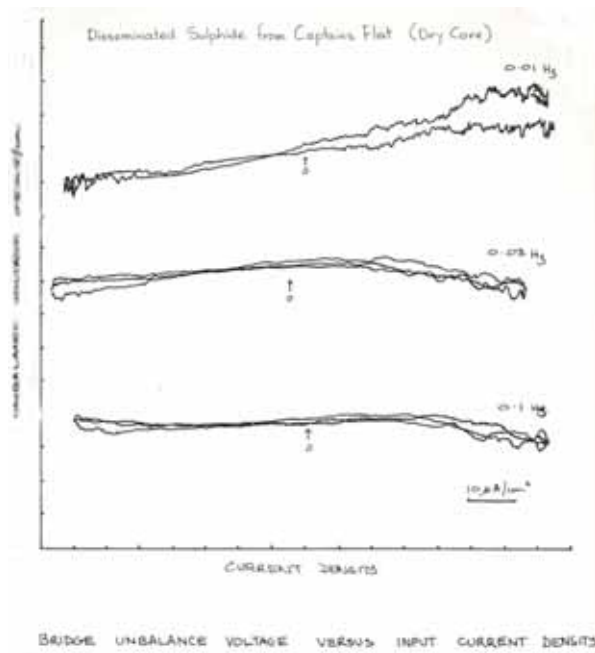


Figure 12. Voltage vs Current, dry core, 10uA.

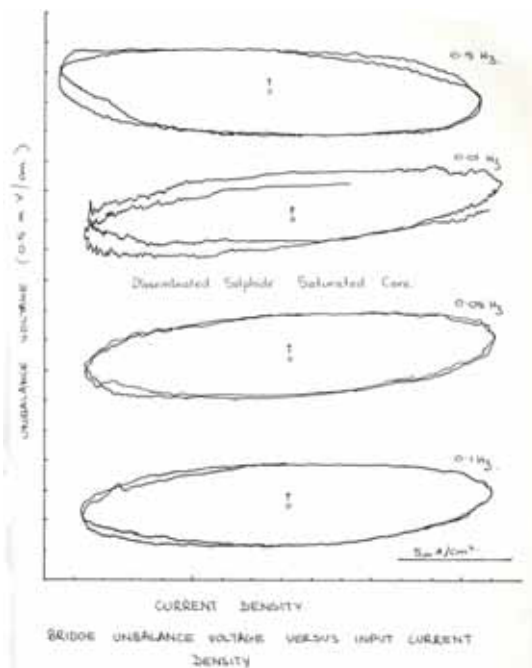
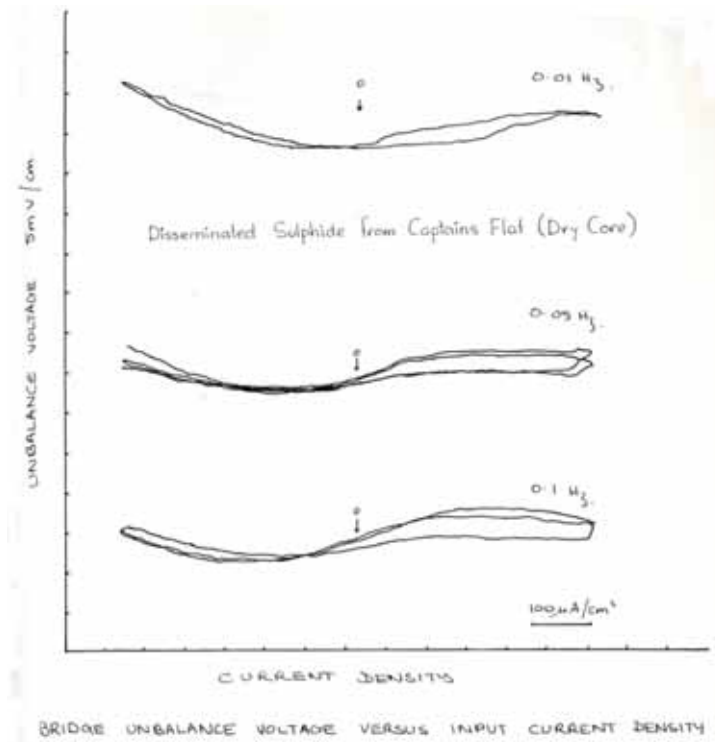


Figure 13. Voltage vs Current, saturated core, 5uA.

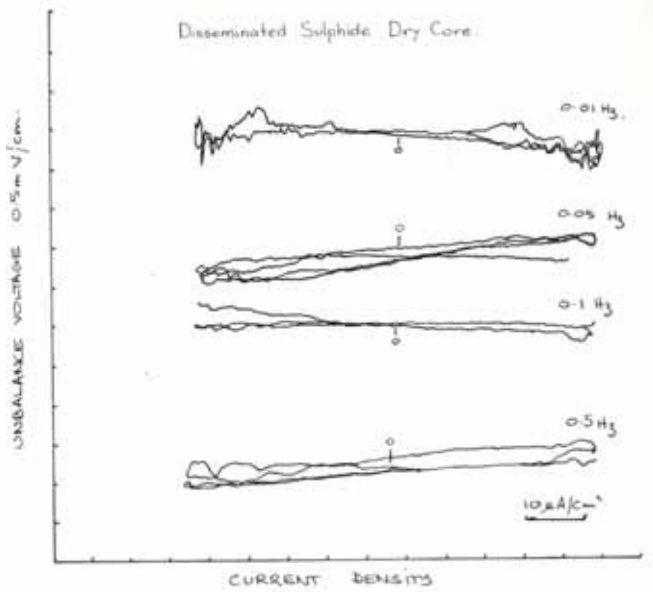


**Figure 14. Voltage vs Current, saturated core, high current density, 100uA.**

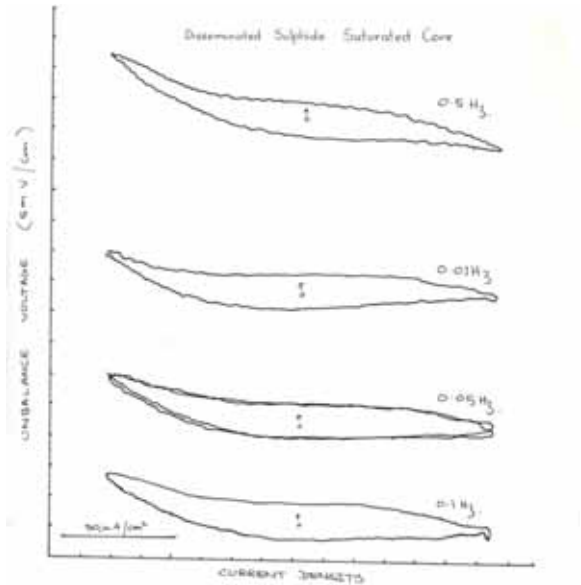
The zero current point on the graph is at a point half way along the x axis of the curve.

At larger current densities the core showed much larger non-linear excursions on the graph (Fig. 13). The hysteresis effect in the curves is probably due to polarization caused by incomplete drying.

When saturated the cores show a large phase shift at low currents ( $\mu\text{A}$ ) due to polarization (Fig. 14). The non-linearity probably still exists in these curves but cannot easily be seen due to the masking effect of the polarization. When higher currents are used ( $100 \mu\text{A}$ ) the polarization does not increase as much as the nonlinearity. The fact that polarization is not linearly proportioned to current density has been noted by other researchers (Anderson and Keller, 1964). This makes it possible to see the effects of the non-linear elements



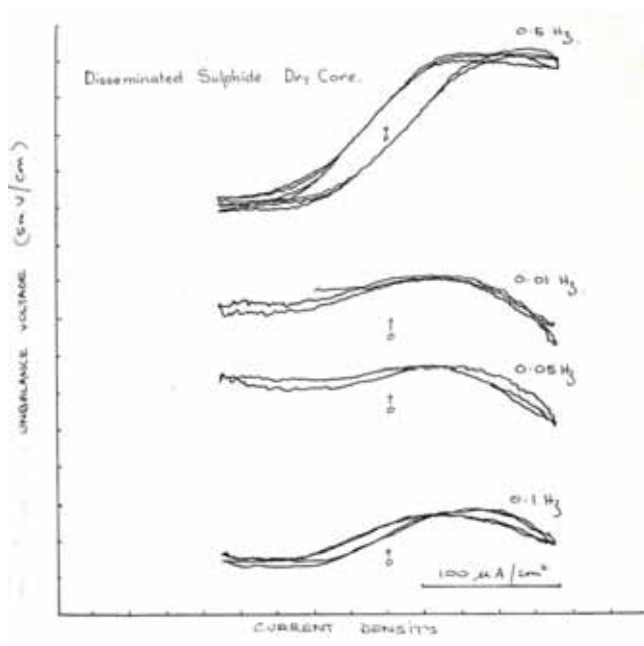
BRIDGE UNBALANCE VOLTAGE VERSUS INPUT CURRENT DENSITY



BRIDGE UNBALANCE VOLTAGE VERSUS INPUT CURRENT DENSITY

**Figure 15. Voltage vs Current, dry core, 10uA.**

**Figure 16. Voltage vs Current, saturated core, 50uA.**



BRIDGE UNBALANCE VOLTAGE VERSUS INPUT CURRENT DENSITY

**Figure 17. Voltage vs Current, dry core, 100uA.**

clearly. (Fig. 15) These effects were quite reproducible when the cores were re-dried and tested again.

It was noticed on a large number of curves that apart from random noise there was a "stepping" superimposed on the curves. This step occurs when the current is increased and also while decreasing, but in the opposite direction as seen in Fig. 18.

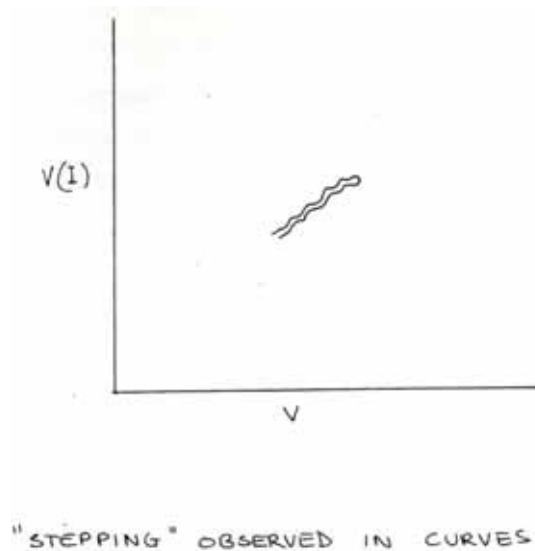


**Figure 18. Voltage “stepping” observed in Curves.**

From the study of these cores the following conclusions can be drawn. The first is that certain non-linear elements exist in rocks containing sulphide mineralisation. Also non-ore bearing rocks appear linear, which could be expected since conduction in these rocks is through the electrolyte present and not through the minerals themselves.

Secondly, the non-linearity increases with current density. It would appear that its increase is not linear.

When testing these rocks the polarization becomes a problem while trying to use currents that approximate field current densities.

The bridge method of measuring the non-linearity has two main disadvantages. The first is a stability or repeatability problem associated with temperature and humidity changes. Both temperature and humidity affect the impedance of the rock sample and unbalance

the bridge causing a drift in the curves obtained. The second is more serious, in that the samples have to be dried before use so that at low currents the polarization does not 'swamp' the non-linearity in the curves. This means that a method of measurement is needed that is more sensitive to non-linear conduction but is less sensitive to effects caused by polarization. After an initial study of the bridge results and their possible interpretation it would appear that the electrolyte played an important part in the electro-chemical reaction that provided the non-linear phenomenon and because some form of electrolyte is usually present in the ground, measurement made in the laboratory would be more meaningful if carried out on saturated samples.

Because of the problems associated with the bridge method of measurements it was proposed to develop a more sensitive method of studying the problem at lower current densities.

### 3.5 DOUBLE FREQUENCY METHOD OF MEASURING NON-LINEAR CONDUCTION.

As discussed earlier any useful exploration method would have to be able to detect non-linearities at current Densities that are encountered in the field. because of the size of the samples in laboratory studies the associated voltages will be small also. The current densities needed for realistic analysis are  $1\mu\text{A}/\text{cm}^2$  and below.

When currents of two different frequencies are passed through a linear network the resultant output will contain only those two frequencies. If a non-linear element is present somewhere in the network then the output contains the original two frequencies, harmonics of the two frequencies, and inter-modulation products of the two frequencies.

In a linear system ohm's law is obeyed.

$$V=IR \quad (26)$$

Where  $V$  is the voltage difference,  $R$  the resistance of the conductor and  $I$  the current through the conductor.

In a non-linear system this relationship no longer holds true. The simplest non-linear system

$$V=IR+A(I) \quad (27)$$

Where  $A$  is a coefficient representing the degree to which it is non-linear.

To represent a more general non-linear case the

$$V = I R + \sum_{n=2}^k (A_n I^n) \quad (28)$$

equation becomes a series.

If two frequencies were used  $\omega_1$  and  $\omega_2$  their currents ( $I_1$  and  $I_2$ ) are

$$I_1 \cos \omega_1 t \text{ and } I_2 \cos \omega_2 t$$

Then

$$\begin{aligned} V \approx & R(I_1 \cos \omega_1 t + I_2 \cos \omega_2 t) \\ & + A_2 (I_1 \cos \omega_1 t + I_2 \cos \omega_2 t)^2 \\ & + A_3 (I_1 \cos \omega_1 t + I_2 \cos \omega_2 t)^3 \\ & + \text{-----} \\ & + A_k (I_1 \cos \omega_1 t + I_2 \cos \omega_2 t)^k \end{aligned} \quad (29)$$

By calculating where all the harmonics and intermodulation products should appear in the spectrum and measuring their amplitudes it should be possible to find some of the above coefficients and by so doing improve our knowledge of the nature of conduction in rocks, especially ores.

Expanding the square and linear term in equation (29)(Appendix B)

$$\begin{aligned} V \approx & R(I_1 \cos \omega_1 t + I_2 \cos \omega_2 t) \\ & + A_2 \{ I_1^2 (\frac{1}{2} + \frac{1}{2} \cos 2\omega_1 t) + I_1 I_2 (\cos (\omega_1 t + \omega_2 t) \\ & + \cos (\omega_1 t - \omega_2 t)) + I_2^2 (\frac{1}{2} + \frac{1}{2} \cos 2\omega_2 t) \} \\ \approx & R I_1 \cos \omega_1 t + R I_2 \cos \omega_2 t \\ & + \frac{1}{2} A_2 I_1^2 \cos 2\omega_1 t + \frac{1}{2} A_2 I_2^2 \cos 2\omega_2 t \\ & + A_2 I_1 I_2 \cos (\omega_1 t + \omega_2 t) + A_2 I_1 I_2 \cos (\omega_1 t - \omega_2 t) \\ & + \frac{1}{2} A_2 (I_1^2 + I_2^2) \end{aligned} \quad (30)$$

This gives the following frequencies and amplitudes:

FREQUENCY	AMPLITUDE
$\omega_1$	$RI_1$
$\omega_2$	$RI_2$
$2\omega_1$	$\frac{1}{2} A_2 I_1^2$
$2\omega_2$	$\frac{1}{2} A_2 I_2^2$
$\omega_1 + \omega_2$	$A_2 I_1 I_2$
$\omega_1 - \omega_2$	$A_2 I_1 I_2$

TABLE 4.

Expanding the cube and linear term in Equation (29)  
(Appendix B)

$$\begin{aligned}
 V = R \{ & I_1 \cos \omega_1 t + I_2 \cos \omega_2 t \} \\
 & + A_3 \left\{ \frac{1}{4} I_1^3 \cos 3\omega_1 t + \frac{1}{4} I_2^3 \cos 3\omega_2 t \right. \\
 & + \frac{3}{4} I_1^3 \cos \omega_1 t + \frac{3}{4} I_2^3 \cos \omega_2 t \\
 & + \frac{3}{2} I_1 I_2 (I_1 + I_2) \\
 & + \frac{3}{4} I_1^2 I_2 (\cos (2\omega_1 t + \omega_2 t) + \cos (2\omega_1 t - \omega_2 t)) \\
 & \left. + \frac{3}{4} I_1 I_2^2 (\cos (\omega_1 t + 2\omega_2 t) + \cos (\omega_1 t - 2\omega_2 t)) \right\} \quad (31)
 \end{aligned}$$

This expansion gives the following frequencies and amplitudes:

Frequency	Amplitude
$\omega_1$	$RI_1 + \frac{3}{4} I_1^3 A_3$
$\omega_2$	$RI_2 + \frac{3}{4} I_2^3 A_3$
$2\omega_1 + \omega_2$	$\frac{3}{4} I_1^2 I_2 A_3$
$2\omega_1 - \omega_2$	$\frac{3}{4} I_1^2 I_2 A_3$
$\omega_1 + 2\omega_2$	$\frac{3}{4} I_1 I_2^2 A_3$
$\omega_1 - 2\omega_2$	$\frac{3}{4} I_1 I_2^2 A_3$
$3\omega_1$	$\frac{1}{4} A_3 I_1^3$
$3\omega_2$	$\frac{1}{4} A_3 I_2^3$

TABLE 5.

To avoid the possibility of spurious results due to the presence of harmonics in the exciting waveforms, it was decided to attempt to measure intermodulation products of the two frequencies.

It can be seen then the best ones to study are likely to be

$$2\omega_1 \pm \omega_2, \quad 2\omega_2 \pm \omega_1, \quad \omega_1 - \omega_2 \quad \text{and} \quad \omega_2 + \omega_1$$

From an instrumental point of view the best frequencies to observe are those furthest away from the source frequencies,  $\omega_1$  and  $\omega_2$ .

Evaluating the co-efficients of Equation 29 would be simplified by a complete spectral analysis of each rock. This would supply enough information to define all of the non-linear parameters involved in the conduction through the rock.

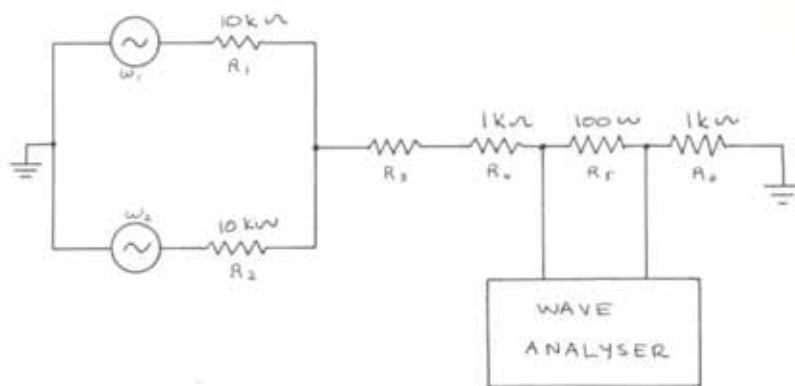
The problem of polarization that hampered the bridge method should have no effect on this new method of study. Wet or saturated cores can, therefore, be used to yield more meaningful results. Samples were prepared using the techniques described for the single frequency method.

### 3.6 METHOD OF MEASUREMENT.

There are many instruments that are capable of measuring spectra or discrete parts of them. One such device tried was a phase sensitive voltmeter. This was used in conjunction with a four electrode system, whose current electrodes were the graphite type previously described. The potential electrodes were graphite painted on in an aqueous solution in the form of two bands, one-third and two-third the way along the core. Results were obtained using this electrode system and the phase sensitive voltmeter. The excitation voltage was derived from two sine wave generators. The phase sensitive voltmeter was referenced with a swept frequency oscillator. The inphase output of the phase sensitive detector was plotted against frequency.

Results were obtained using the system but the nonlinearity detected appeared, at least in part, to be due to the phase sensitive voltmeter. Two makes of voltmeter gave similar results. In an attempt to overcome this, two notch filters were built to remove the carrier,  $\omega_1$  and modulator,  $\omega_2$ . The results were slightly better but drift in the high 'Q' filters proved to be high and caused considerable trouble. This system, even when tested using wire wound resistors replacing the rock, produced intermodulation products. A study of measuring technique showed that a spectrum analyser or wave analyser was probably the best instrument to use. These instruments are designed for this type of measurement, that is measuring intermodulation products in radio signals. The only difference is that the present problem required an instrument that operated in the low audio range. A wave analyser (General Radio model 736A) was used in the present testing program. (Unless otherwise stated all A.C. currents and voltages are R.M.S. values.)

This instrument was tested with a 300 mV input, using the set-up in Fig. 19, and gave intermodulation products that were at least 70 dB down on the input. All the resistors used were wire wound, and the network  $R_4$ ,  $R_5$  and  $R_6$  (Fig. 19) represented the rock.



CIRCUIT USED TO TEST WAVE ANALYSER.

**Figure 19. Circuit used to test the Wave Analyser.**

The wave analyser was not equipped with a pre-amplifier, so for maximum resolution the input signal (total) has to be 300mV R.M.S. This necessitated the building of two linear, low noise pre-amplifiers, to allow for low current density measurements. Both amplifiers were designed with differential input. One had a fixed voltage gain of 5000 and an input impedance of  $1\text{M}\Omega$ . With this pre-amplifier, considerable trouble was taken in matching components to keep the circuit linear. (See Appendix A).

The other preamplifier had variable gain and an input impedance of  $20\text{m}\Omega$  operational amplifiers to achieve gain control and high input impedance, and had voltage gains of 0.5 to 3000 in 8 switchable settings (see Appendix A). An input impedance of  $10^9\ \Omega$  (D.C.) is possible with this amplifier but  $20\text{M}\Omega$  was found to be adequate when using saturated cores. It had a frequency response of 5hz to 10Khz.

Some preliminary measurements were made using the equipment set-up in Fig. 20.

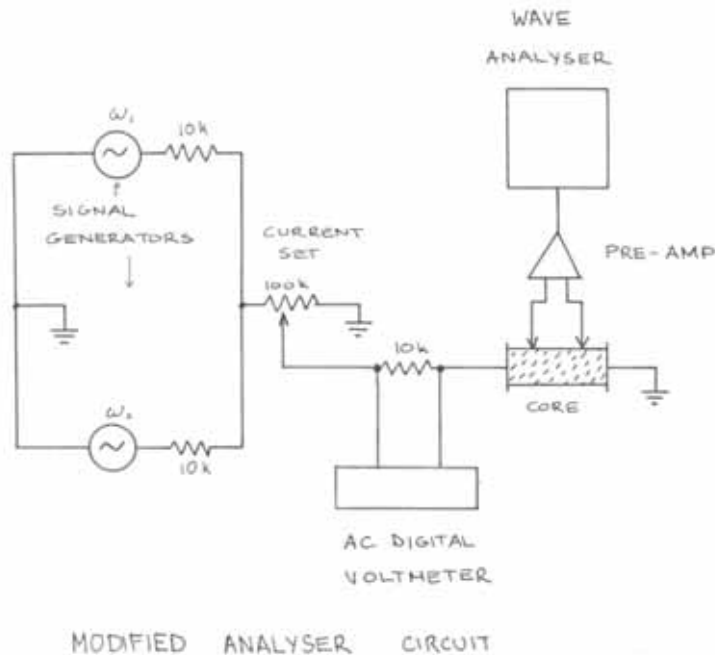


**Figure 20. Modified measuring circuit.**

A sandstone sample saturated with tap water ( $73\Omega\text{m}$ ) gave no measurable I.M. products (i.e. less than 70dB) even with current densities of several milliamps/cm<sup>2</sup>. This showed that the measuring system had no significant inherent non-linearities.

A disseminated sulphide core was then tested. The core contained mainly pyrite with minor amounts of chalcopyrite, the total sulphides being about 30%. The rock was saturated with the same electrolyte as the sandstone. This core gave surprisingly low I.M. products, down about 70 dB. The voltage across the potential electrodes was very low so high gains had to be used, which gave very noisy signals. These results were generally inconclusive, except that the I.M. products were low.

To improve accuracy more voltage output was needed from the rock. Since the current flow through the rock is non-linear, then the voltage drop across a resistor in series with the rock can be used to monitor the I.M. products. This eliminated the two electrodes around the core, making sample preparation simpler, and allowing the core to be covered by insulating tape which greatly reduces drying out during testing.

A series of tests using disseminated sulphide cores and sulphide free cores were carried out using this system. The sulphide free cores gave no detectable I.M. products up to hundred of micro amps/cm<sup>2</sup>. The disseminated sulphide cores gave very low I.M. products, but were rather more noisy than the non-mineralised samples. The noise appeared to be originating from the rock rather than the system. before further testing was carried out the system was further modified to allow a D.C. bias to be placed across the rock sample in either direction. Fig. 21 shows schematics of the circuits used for all subsequent testing.

The high impedance circuit was used in testing, most of the cores having an impedance of  $> 1\text{k}\Omega$  (usually around  $2\text{k}\Omega$ ). The measurements were carried out in an earthed aluminium box  $1\text{m}^3$ . The preamp box and the current control box were also earthed so considerable care had to be taken to avoid earth loops. An oscilloscope was used to monitor the output of the preamp. In all testing carried out, the amplitudes of the  $\omega_1$  and  $\omega_2$  were the same.

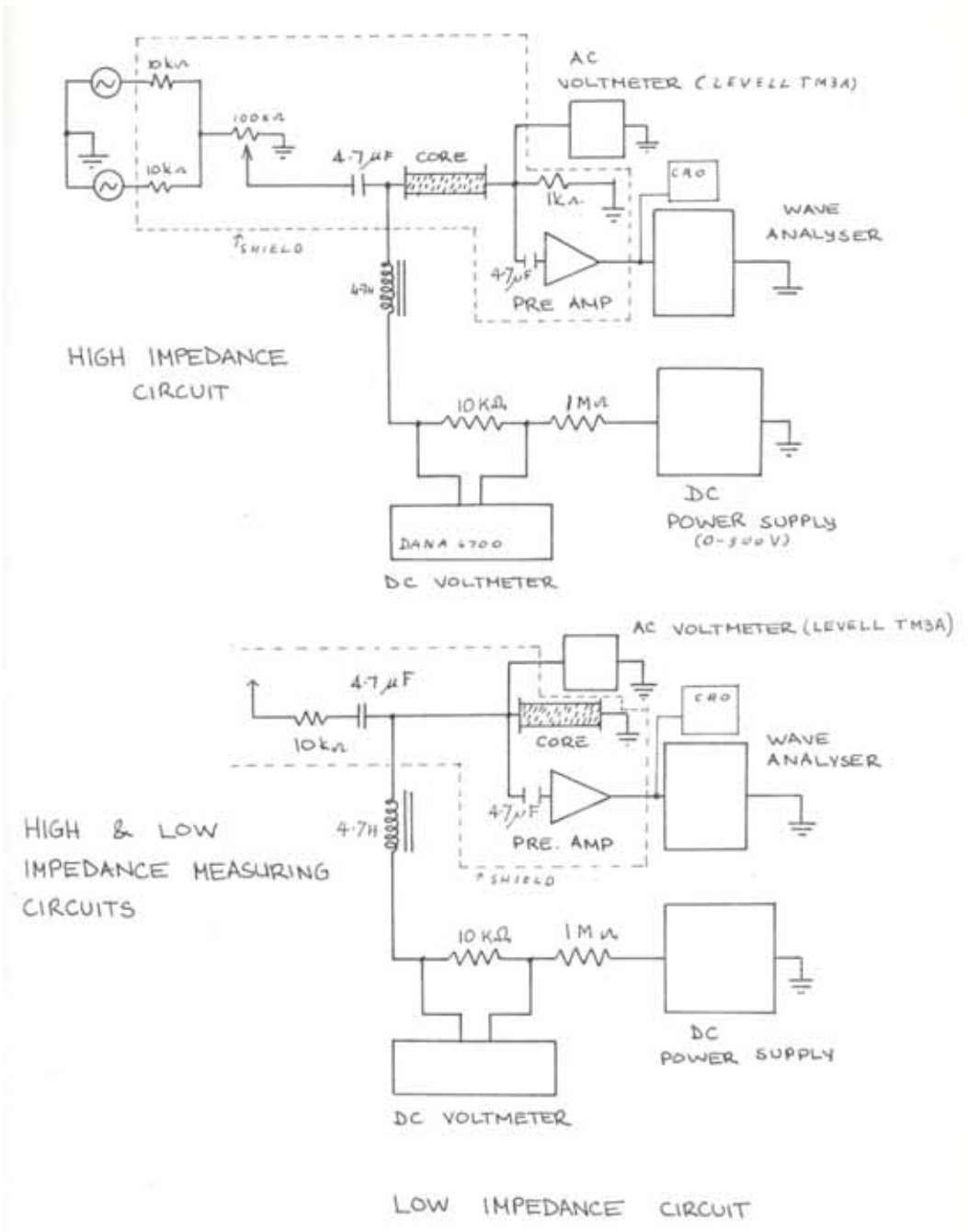


**Figure 21. Schematics of the circuits used for all subsequent testing.**

### 3.7 RESULTS.

Three main rock types were used in testing. The first was a relatively clean Hawkesbury sandstone from Ryde, NSW. This sandstone was used to test for system linearity. When dried, the impedance of the sample was well over 200 Megohms. The rock was then saturated with tap water ( $73\Omega\text{-m}$ ). This reduced the resistivity of the rock to just above that of the saturating electrolyte.

The next set of rocks were Cu-Pb-Zn sulphides from Woodlawn, N.S.W. The massive sulphide ore contains generally about 75% of total sulphides, consisting of pyrite, sphalerite, galena and chalcopyrite in order of decreasing abundance, plus probably less than 1% of tetrahedrite - tennantite, arsenopyrite, pyrrotite and stannite. The ore is fine-grained and finely to coarsely banded.

The other are type used was from Captains Flat, N.S.W. This are shows primary banding, the outcome of progressive replacement of a schistose rock. It is a Cu-Pb-Zn are. The copper concentrations are irregularly distributed through the lead-zinc are. Apart from very small amounts of gold, the ore contains pyrite, tennantite, arsenopyrite, and chalcopyrite. The pyrite forms as a halo around the body and into the host rock for a considerable distance. Most of the ore is massive, with very little dissemination around the edge.

The frequencies used in this work were 70 Hz and 56 Hz. These were chosen on a number of criteria. The first was to keep the frequencies low, as any future field work would have to be done at low frequencies; also an early Russian paper (Shaub et al. 1971) noted that the non-linear effect seemed to diminish with increasing frequency. The frequencies were chosen so that the primary harmonics of the frequencies used did not lie on or near the expected intermodulation products or mains harmonics. Fig. 22 is the wave form used. Table 6 shows the primary frequency harmonics and intermodulation products in the range of interest.

	<u>FREQUENCY Hz</u>	
$\omega_1$	56	
$\omega_2$	70	
$2\omega_1$	112	Frequencies used in present study and their products.
$\omega_1 + \omega_2$	126	
$2\omega_2$	140	
Mains	150	
$2\omega_1 + \omega_2$	182	
$2\omega_2 + \omega_1$	196	

TABLE 6.

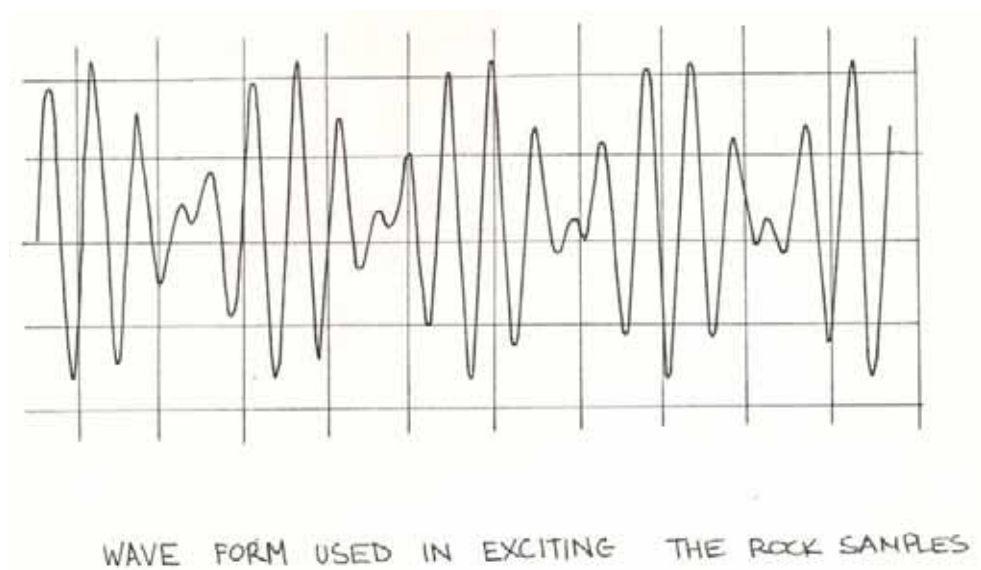


**Figure 22. Waveform used in Exciting the Rock Samples**

The best frequency for study was found to be 126 Hz because it appeared to be the largest of the I.M. products. It is also sufficiently separated from the 70 Hz carrier for interference to be negligible.

Sandstone was one of the first samples tested since it should produce no intermodulation (IM) products. The conduction through sandstone should be only through its saturating electrolyte and not through the

host mineral which is far more resistive. Sandstone produced no detectable I.M. products with current densities up to several milliamps/cm<sup>2</sup>, even with a D.C. bias. Repeated measurements of the sandstone sample were used to keep check of the equipment during the remainder of the testing.

Several samples of rock from Captains Flat containing from 5% to 60% sulphide were tested using no D.C. bias. Only in the hundreds of μA/cm<sup>2</sup> range was there any sign of non-linearity present. This was still well within the noise region of measurement and no positive results could be obtained.

The results using a D.C. bias were much more encouraging. Fig. 23 shows the results using a disseminated sulphide from Captains Flat. This rock contained about 10% sulphide concentrated in blebs of the order of 1mm across. The graph is a plot using constant D.C. bias while varying the A.C. signal input. The A.C. current density is plotted against the ratio of the voltage output at 126 Hz ( $\omega_1 + \omega_2$ ) and the total voltage out, multiplied x 10<sup>3</sup>, i.e.

$$x = \frac{\text{Voltage at 126 Hz} \times 10^3}{\text{Total voltage out}}$$

Most of the graphs shown are presented in this way.

Fig. 23 shows the plot of zero D.C. bias and 1.3μA/cm<sup>2</sup> bias using both positive and negative biasing. There is a marked increase in the intermodulation product (I.M.) with an increase in D.C. bias current. The turnover of the graphs at 0.26μA/cm<sup>2</sup> is because the I.M. product has dropped into the noise level region and the total output voltage continues to get smaller while the I.M. reading remains the same.

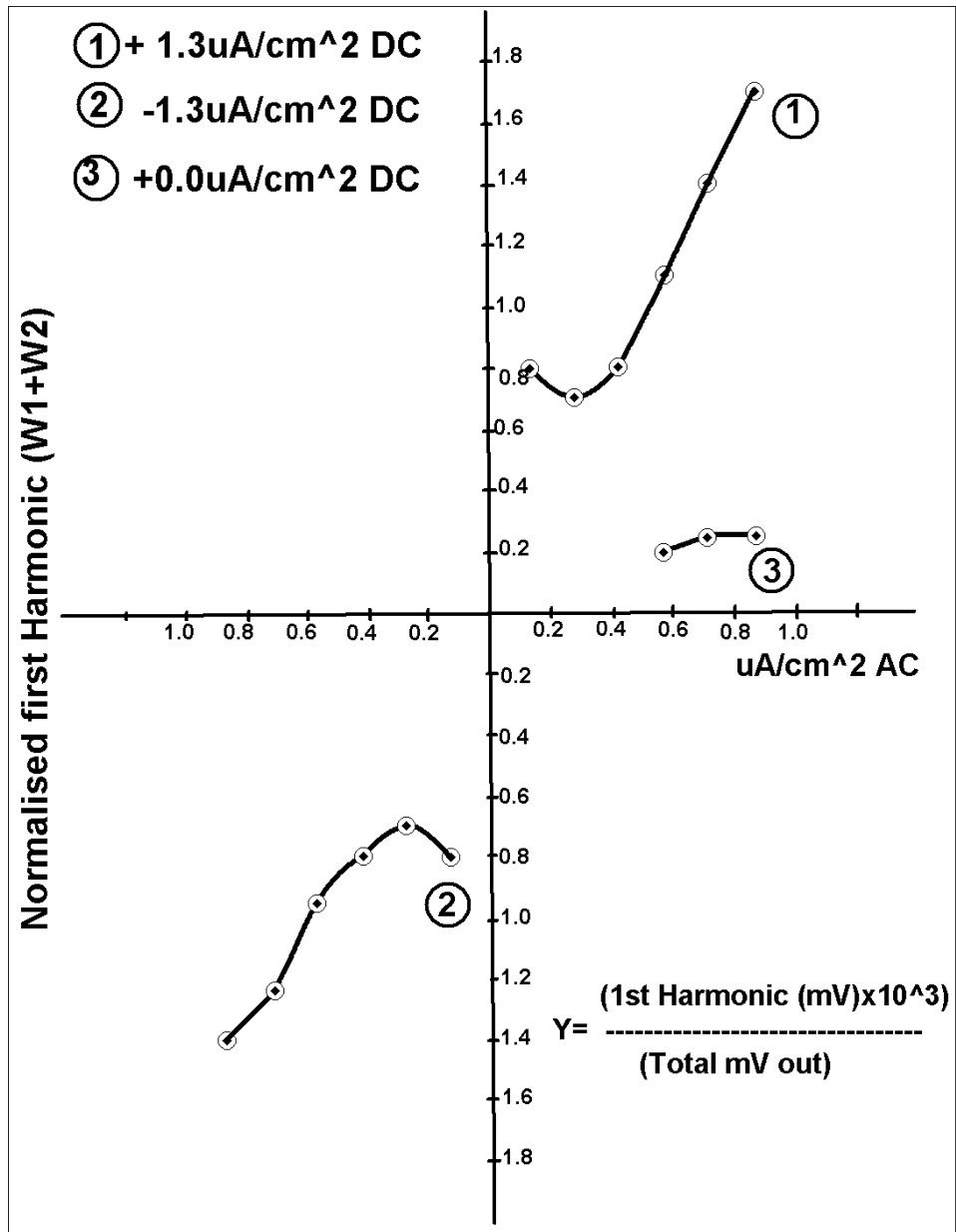


Figure 23. First harmonic verses DC bias change.

Fig. 24 is for the same rock but at higher current densities. The D.C. currents are  $\pm 1.3\mu\text{A}/\text{cm}^2$  and  $\pm 2.6\mu\text{A}/\text{cm}^2$ . The negative D.C. biased cores do not give the same results as the positively biased ones. This non-reversibility of the curves was noted to varying degrees in all of the tests done.

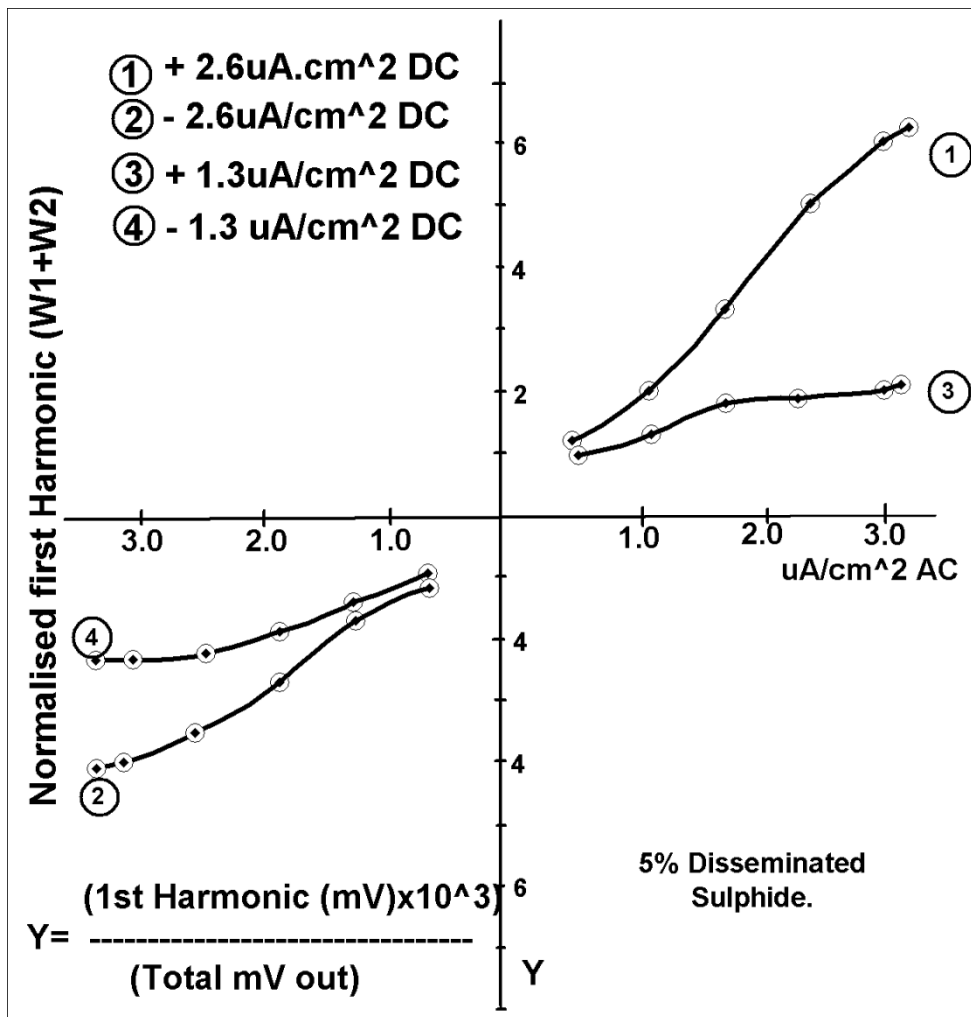
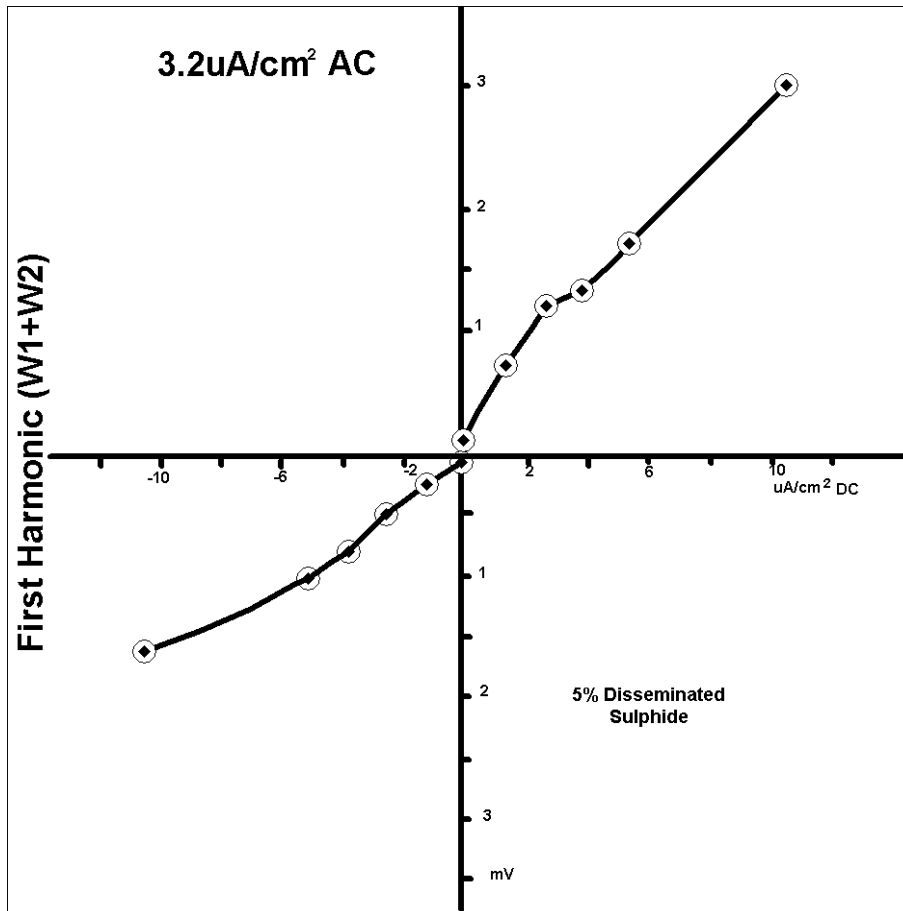


Figure 24. First harmonic versus DC bias change, at higher AC currents.

A plot using constant A.C. current input against varying D.C. Bias is shown in Figure. 25. This has many of the same features as the previous curves with the curve for negative D.C. bias being different from the positive curve. Note that this curve is D.C. current density plotted against mV of the intermodulation product ( $\omega_1 + \omega_2$ ) since the total voltage out remains the same. The A.C. current density in this case is  $3.2\mu\text{A}/\text{cm}^2$ .

Analysing these results we note a number of things. The first is an increase in the non-linearity with an increase in direct current bias. This increase in non-linearity is quite marked, a doubling in bias current more than doubling the non-linear output plotted.

Another feature seen is the difference in output with opposite polarities of the D.C. bias. This appears to be connected with another phenomenon that was noted, that is the non-linear output varied with time. If the rock was left with both alternating and direct current passing through it, the non-linear output decreased with time in the order of minutes. The current flowing through the rock seemed to decrease very slightly but this may have been due to instrumental drift.



**Figure 25. First harmonic, constant AC and variable bias.**

This variation of the non-linearity with time means that the results are not exactly repeatable. It was noted that if constant direct and alternating currents were passed through the rock for a period of five minutes, and then the D.C. bias reversed, the non-linearity in this reversed direction had increased considerably. The increase depended on the length of time that the current had been flowing in the other direction. If the current was again reversed, with both direct and alternating currents at the same value as before, the non-linear output again changed considerably. This phenomenon caused considerable trouble before it was recognised. Until the dependence on time was noted it was presumed that the non-repeatability was due to experimental error.

Several other samples were also tested but due to unrepeatability were not fully recorded since at the time it was felt the results were in error.

These results did however contain much the same features as the results presented so that the conclusions that are drawn are not done on only a very limited number of cores.

#### **4. DISCUSSION OF RESULTS.**

In an attempt to explain the results obtained, methods of conduction in semi-conductors were examined more closely.

A depletion layer exists in the region of the contact between a p and an n-type semi-conductor. In the depletion layer equilibrium is approached, that is there is no excess of holes or electrons, due to recombination.

Similarly, a depletion layer can be formed when an n-type material comes into contact with an n<sup>+</sup> type material. This depletion region will not be at zero potential, but there will still be a potential gradient between the n and n<sup>+</sup> material, as in Fig. 26.

The n<sup>+</sup> material can be created by different doping levels within the same material or by different n-type materials. Either situation could very easily occur in Natural minerals where different minerals are often in contact or where impurity levels within the same minerals vary. These n - n<sup>+</sup> junctions, although not rectifying, are non-linear.

Another junction that is probably of lesser importance is the Schottky barrier rectifier. Here n type material comes into contact with a metal. Consider an electron going from left to right, in Fig. 27. It must acquire energy which is the contact potential between the two regions, hence electrons diffuse from left to right until the depletion region shown in Fig. 27 is formed.

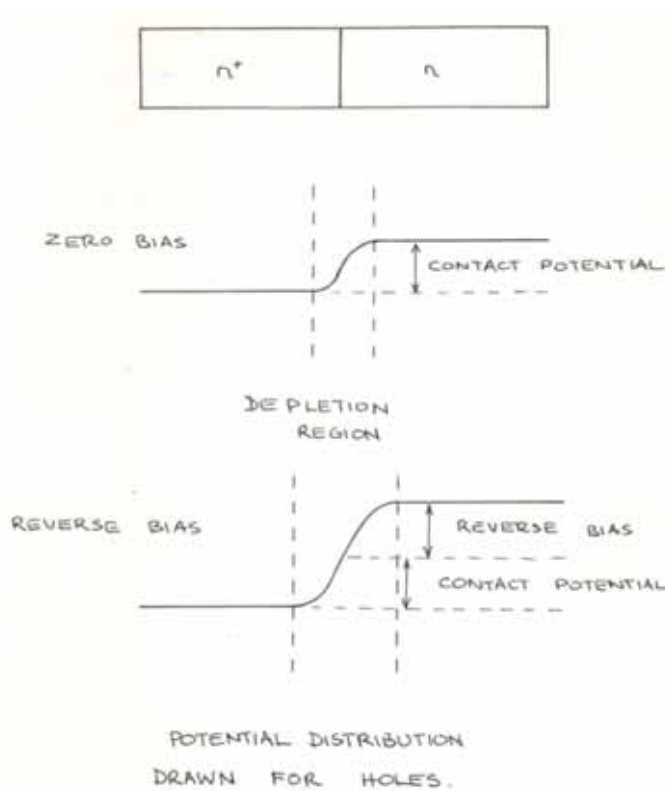


**Figure 26. Potential distribution across n - n<sup>+</sup> junction.**

When a reverse bias is applied, for an electron to go from left to right it must not only overcome the contact potential  $\phi$ , but also the reverse bias  $V_r$ . (Fig. 28).

This type of junction is only applicable in natural minerals where elemental metals such as gold, copper or silver are present. They can occur in varying quantities in some ore bodies.

In Chapter 3, using the single frequency method, a stepping type of curve was noted. These curves also contain a lot of noise that appeared to originate from within the rock. The noise and its possible explanation will be discussed first.

Chapter 2 showed that in a semi-conductor two main energy bands exist, the conduction band and the valence band. An imperfect lattice generates intermediate levels in the forbidden energy gap or band, and these act as

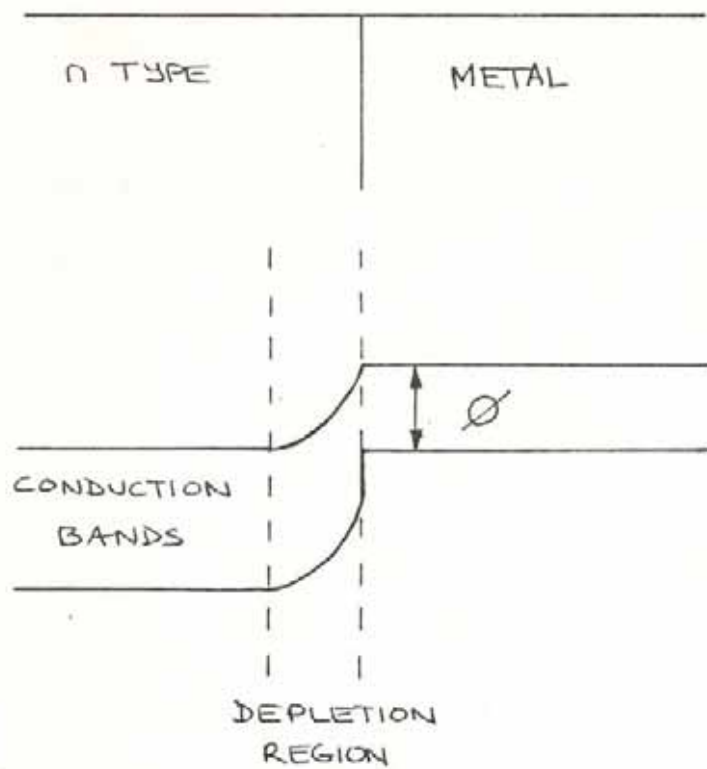


**Figure 27. Energy bands for Schottky Diodes.**

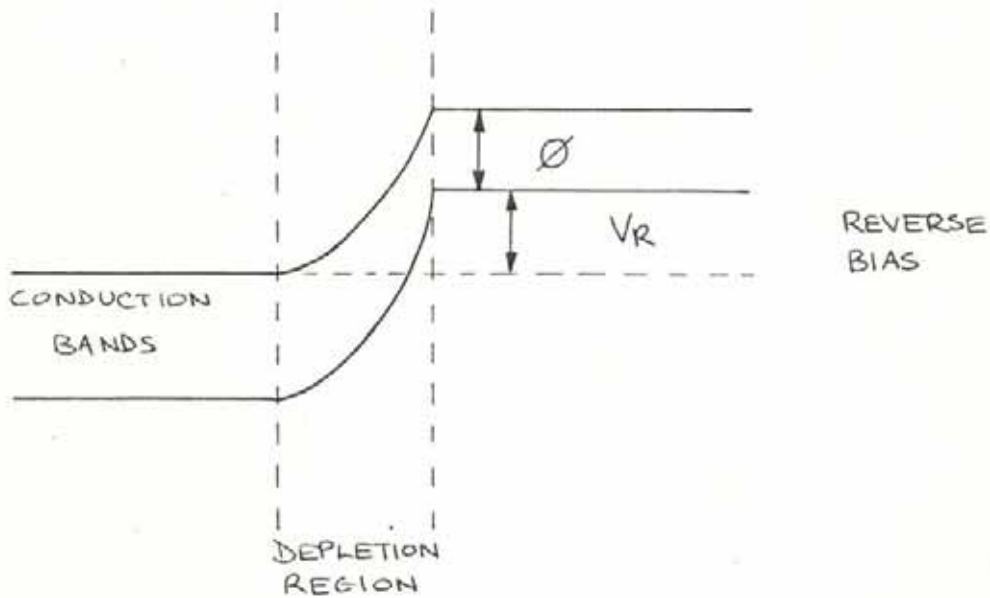


**Figure 28. Energy bands for Schottky Diodes with reverse bias.**

"stepping stones" for the electrons to hop from the valence to the conduction band. These intermediate levels will obviously predominate at the surface where the lattice terminates and the possibility of dislocations is highest.

If the dislocations result in energy levels close to the conduction or valence bands the probability of the electron hopping from the valence to the dislocation and back to the valence band is quite high. The same applies to the conduction band. This dislocation is most effective in recombination, if it is near the centre of the forbidden energy band, like a stepping stone in the centre of a stream. This produces noise which has an inverse frequency dependence ( $f^{-1}$ ). If the semiconductor is carrying a current then recombination and generation vary the current in an impulsive manner.

The stepping seen in these curves could be due to electron hopping where, on the application of a current, the electrons hop from the valence band to the conduction band via dislocation or impurity levels in the forbidden band. This would cause sudden increases in the conduction causing the steps observed.

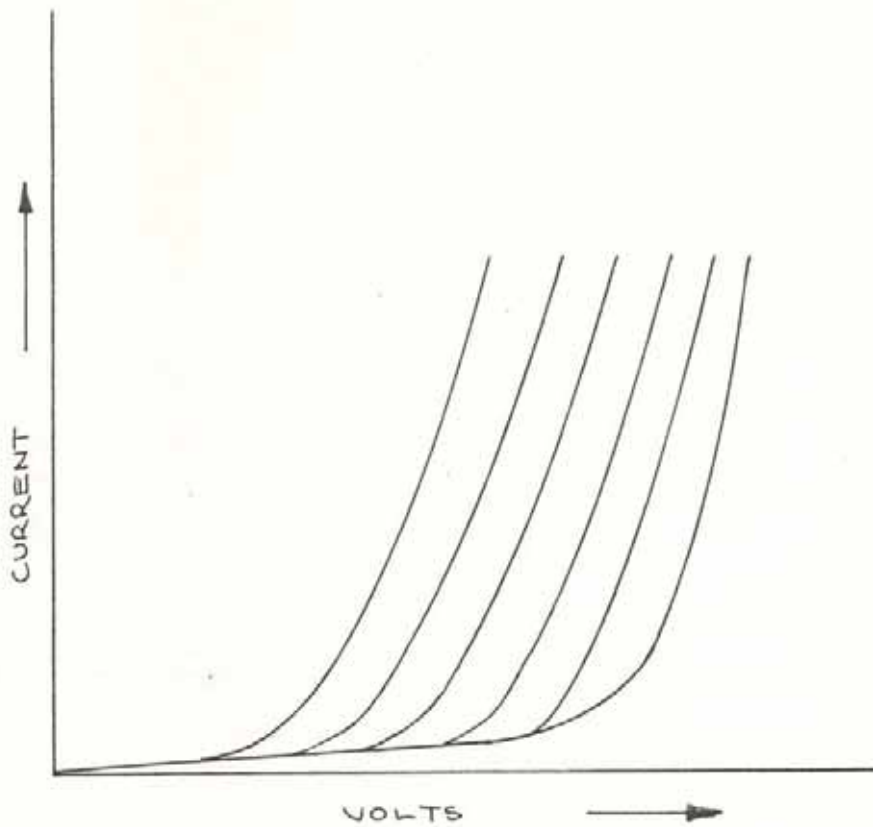
A more probable explanation is that various junctions are switching on due to the rising voltage so that the current increases in steps. These junctions do not switch on until the potential applied has risen over the contact potential. The contact potential depends upon the doping levels within the materials involved, so if a number of different materials were in contact it would produce a series of current-voltage characteristic curves as in Fig. 29.

These would produce the current voltage curves observed, that is sudden jumps in current flow with an increasing voltage.

The effect that D.C. bias has on the double frequency curves can be explained in terms of biasing. This reverse biasing has two effects. The first is that it turns more junctions 'on'. Secondly, it makes the junctions

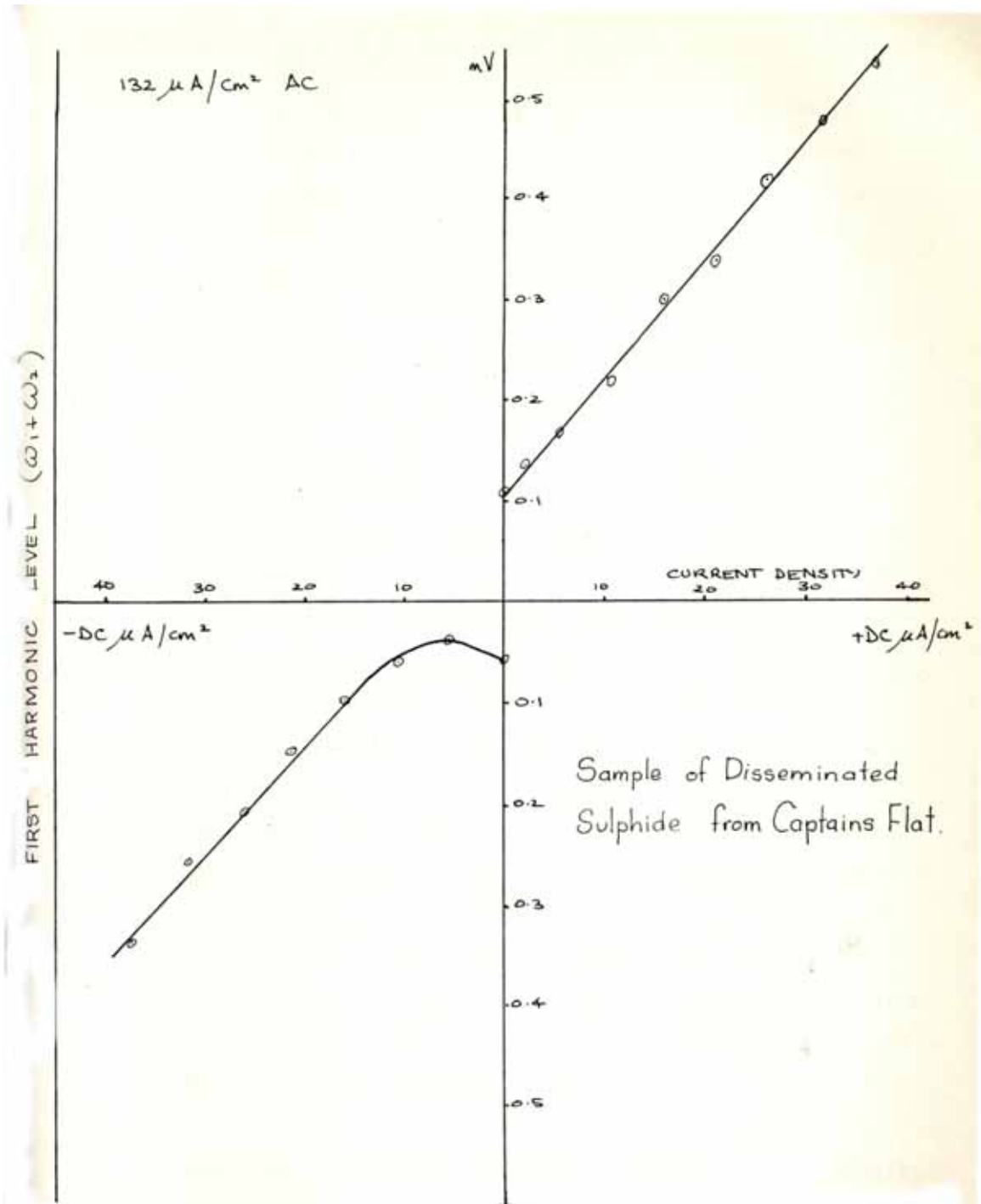
operate in a steeper portion of their voltage-current curve. It must also be realized that this same biasing turns just as many diodes 'off' since their orientation is random. Its main effect though is to get the conduction up onto the steeper and more non-linear portion of the curve. This greatly increases the non-linear behaviour. Fig. 25 clearly shows the effect of this bias.

Fig. 30 shows the effect of a Direct Current bias on a core (5% sulphide from Captains Flat). This core contained less sulphide than that used to obtain the results of Fig. 25, and is correspondingly more linear. Some odd effects can be seen on the negatively biased curve. These were caused by leaving the bias on approximately five minutes before taking measurements.



VOLTAGE - CURRENT CHARACTERISTIC CURVES FOR DIFFERENT DOPING LEVELS

**Figure 29. Voltage/Current characteristics for different doping levels.**



**Figure 30. First harmonic verses DC bias change, at higher DC & AC currents.**

When a current is passed across a sulphide-electrolyte interface  $H^+$  ions are forced into solution at one side of the sulphide grain. Since most groundwater contains  $Cl^-$  ions there will be a tendency for  $HCl$  to form. This  $HCl$  will etch the sulphide surface and also leave various secondary products on the interface. These deposits may build up with time, thus changing the nature of the surface of the sulphide. Since most of the conduction effects are surface effects the conduction pattern will change with time. If the current flow is reversed then this etching will take place on the opposing face. Upon reverting to the original direction after a period of time the form of conduction will generally be different from the original one since conditions at the interfaces have changed. This effect is probably not noticeable in most other methods, such as induced polarization, since the currents do not flow in anyone direction long enough for the above processes to take effect.

Sill (1963) discusses electrode noise and possible causes. He was mainly concerned with metal-electrolyte interfaces.

He noted that this noise had a near inverse frequency power spectrum. The sources of this noise were thermal noise, shot noise, current modulation noise and noise due to fluctuations in thermodynamic quantities.

In chapter 2, equation (17), for the current flow across a p-n junction was derived:

$$J = (J_{e0} + J_{h0}) (e^{eV/kT} - 1)$$

Figure 31 shows the current-voltage characteristic of a p-n junction according to equation (17). This equation will be examined more closely in an attempt to get a better feeling for the voltage levels and current densities involved. The first point to note is that most of the potential drop will occur across the depletion region, since the resistivities of the bulk materials are low.

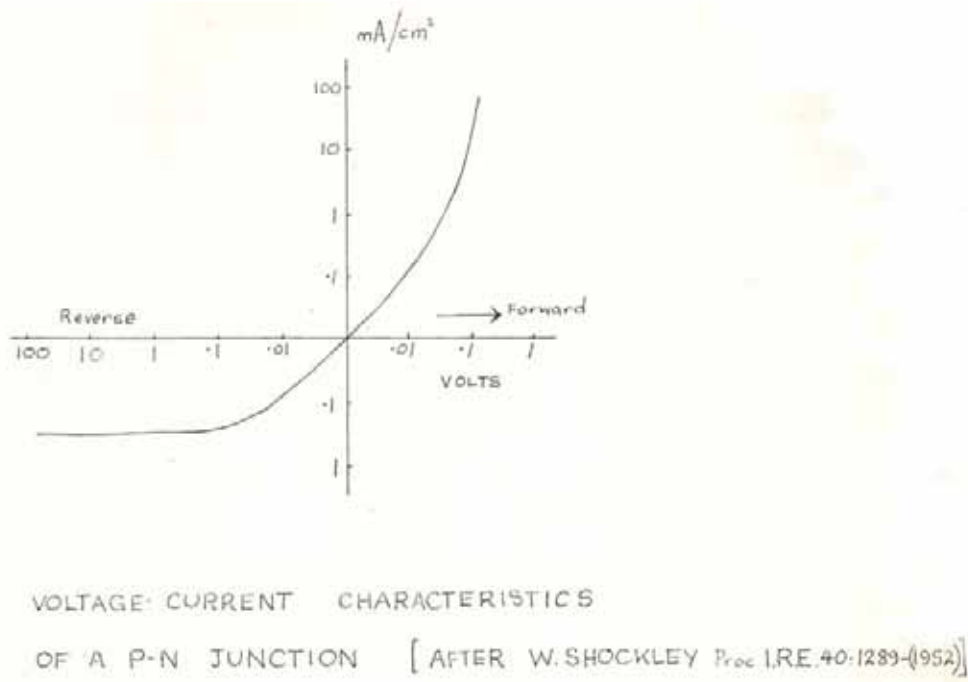


**Figure 31. Voltage current characteristics of a p-n junction.**

From equation (17) the shape of the current-voltage curve is fixed but the numerical values vary according to the values of  $J_{e0}$  and  $J_{h0}$ . Equation (17) can be rewritten:

$$J = e \left( \frac{D_e N_{e0}}{L_e} + \frac{D_h N_{h0}}{L_h} \right) (e^{eV/kT} - 1) \quad (32)$$

Where  $L_e$  is the diffusion length of electrons in the p region,  $L_h$  is the diffusion length of holes in the n region,  $N_{e0}$  is the density of Electrons in p-type material in thermal equilibrium,  $N_{h0}$  is the density of holes in n-type material in thermal equilibrium and  $D_e$  and  $D_h$  are diffusion constants which are proportional to mobility.

To calculate the current density involved in conduction, the density and mobility of majority and minority carriers for both materials must be known, as well as temperature. Since the exact chemical composition of the materials involved, including impurity levels, are unknown it is not possible to put exact figures on the current densities and voltage gradients involved in naturally occurring rocks. A more detailed

explanation of the processes involved can be found in a book by A.J. Dekker (1961).

No region of Fig. 31 is linear although some portions of the curve show greater non-linearity than others. It was noted earlier that the direct current bias had the effect of forcing the A.C. conduction to take place along a less linear portion of the voltage-current curve since the central portion (around zero) of the curve is more linear than elsewhere on the curve.

The possibility that the effects observed came from sources other than solid-solid interfaces cannot be completely ignored. Madden (1961, p.43) "observed in practice that the impedances are linear for current densities of  $10^{-7}$  amps/ $\text{Cm}^2$  or less at low frequencies (.01 Hz). At higher frequencies more current can be passed without any appreciable non-linearity"

## 5. CONCLUSION.

The most effective method found of studying non-linear effects in mineralized rocks is the double frequency method with a direct current bias. The single frequency method is only useful when using high current densities and dry cores.

Using the dual frequency method a stable filter is needed to detect the intermodulation products. The characteristics of the wave analyser were found to be adequate.

No measurable non-linearity was detected on the non-mineralized samples tested. The non-linearity of mineralized cores was small when no direct current bias was used (<1%). The non-linearity increased as much as five times when a direct current bias was used. The nonlinearity varied from sample to sample but insufficient samples were studied to see if these curves were diagnostic of individual minerals or mineral assemblages.

These non-linear properties are thought to be due to non-ohmic contacts of differently doped material. The majority of these contacts are non-rectifying but this does not imply that they conduct in a linear manner.

The contacts are probably of the  $n - n^+$  or  $p - p^+$  type rather than the conventional p-n junction, but they still have several of the properties of the p-n junction.

A direct current bias has approximately the same effect on both types of junctions, that is it helps to turn them on or off. This bias forces the A.C. conduction to take place on a less linear portion of the voltage-current curve, greatly enhancing the non-linear output.

There are two types of rock dependent noise, one that depends on applied voltage gradients and another that is frequency dependant. The first type of noise is caused by each junction turning on and off with varying voltage gradients. The second type of noise varies

approximately as  $f^{-1}$ . Certain features of this type of noise were discussed by Sill (1963). As was discussed earlier it may be caused by electrons jumping in and out of the conduction band.

The observed results were in the order of 60 dB down on the total received signals. This means that, in terms of the conduction equations in Chapter 3 and also most present electrical and electromagnetic methods presently employed, the non-linear term associated with conduction in ore minerals can be ignored. It is however large enough to be of significance in mineral detection.

## 6. FUTURE WORK

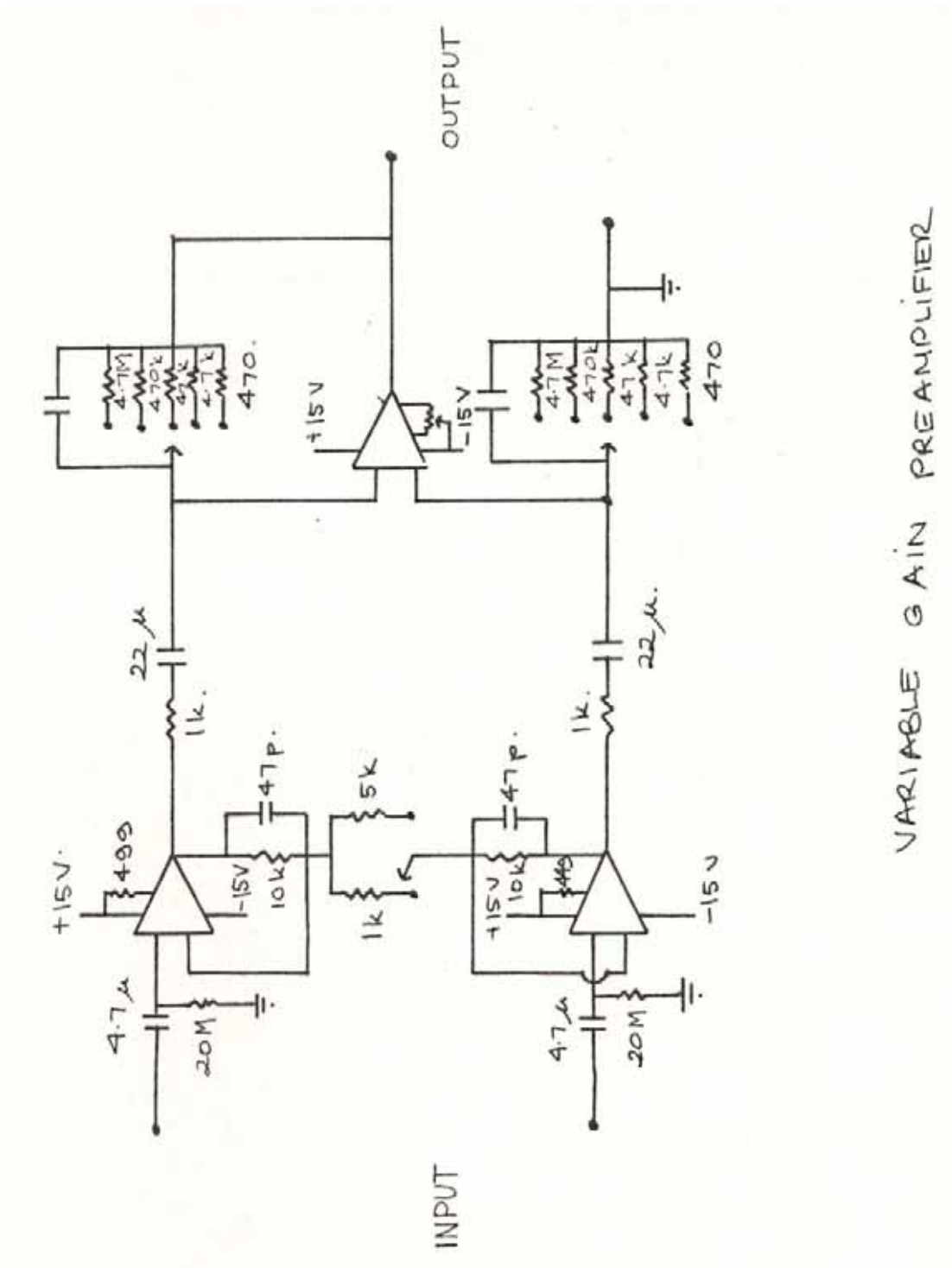
More detailed work is needed on this double frequency method of studying non-linearity of electrical conduction in mineralized rocks. A study is needed on frequency dependence, that is, does the effect get larger or smaller with frequency increase. Included in any future work should be an attempt to isolate the exact cause of nonlinear conduction. Along with this work is needed a standardised method of describing results in relation to the three input parameters.

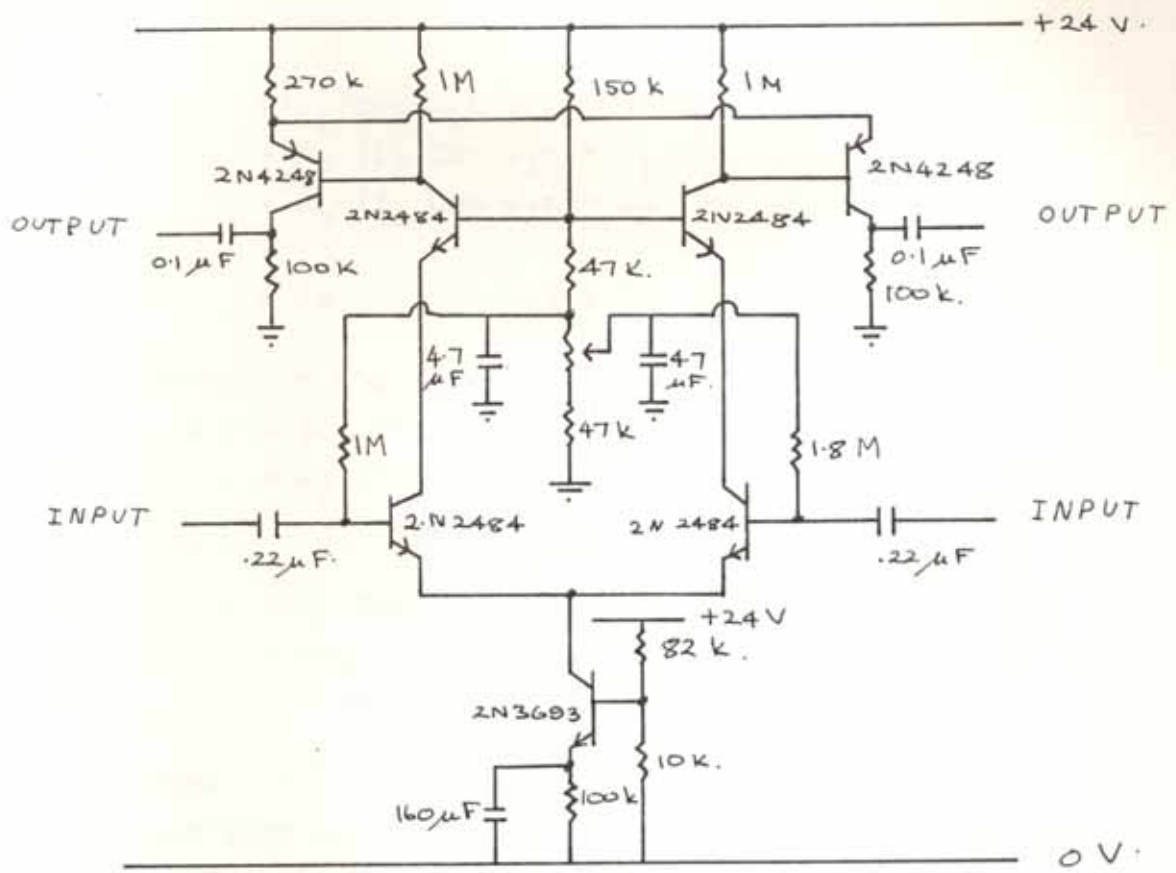
When more is known about the non-linear properties of minerals considerable time should be spent in studying individual minerals and suites of natural and artificial mineral assemblages in an attempt to isolate diagnostic features which may exist. This could involve the study of other intermodulation products within the spectrum.

A study of the effect and use of the direct current bias could prove extremely useful especially when trying to extend the work for use in the field. Without the aid of a D.C. bias the method would probably only be of practical use as a borehole tool.

It may be possible to carry out simple field tests using two 240 volt 50 Hz generators and detuning them, one to about 45 Hz and the other 56 Hz. A D.C. bias could be provided by using wet cell car batteries.

# APPENDIX A





FIXED GAIN PREAMPLIFIER.

## APPENDIX B

### APPENDIX B

A more complete expansion of Equation 29 is presented here.

$$\begin{aligned}
 V = & R(I_1 \cos \omega_1 t + I_2 \cos \omega_2 t) \\
 & + A_2 (I_1 \cos \omega_1 t + I_2 \cos \omega_2 t)^2 \\
 & + A_3 (I_1 \cos \omega_1 t + I_2 \cos \omega_2 t)^3 \\
 & + A_x (I_1 \cos \omega_1 t + I_2 \cos \omega_2 t)^x \qquad (29)
 \end{aligned}$$

Expanding the square term

$$\begin{aligned}
 V = & R (I_1 \cos \omega_1 t + I_2 \cos \omega_2 t) \\
 & + A_2 (I_1^2 \cos^2 \omega_1 t + 2I_1 I_2 \cos \omega_1 t \cos \omega_2 t \\
 & \quad + I_2^2 \cos^2 \omega_2 t) \\
 = & (RI_1 \cos \omega_1 t + A_2 I_1^2 \cos^2 \omega_1 t) \\
 & + RI_2 \cos \omega_2 t + A_2 I_2^2 \cos^2 \omega_2 t \\
 & + 2A_2 I_1 I_2 \cos \omega_1 t \cos \omega_2 t
 \end{aligned}$$

Since  $\cos A \cos B = \frac{1}{2} \{ \cos (A+B) + \cos (A-B) \}$

the last line can be rewritten

$$\begin{aligned}
 & A_2 I_1 I_2 \{ \cos (\omega_1 t + \omega_2 t) + \cos (\omega_1 t - \omega_2 t) \} \\
 V = & \cos \omega_1 t \{ RI_1 + A_2 I_1^2 \cos \omega_1 t \} \\
 & + \cos \omega_2 t \{ RI_2 + A_2 I_2^2 \cos \omega_2 t \} \\
 & + A_2 I_1 I_2 \{ \cos (\omega_1 t + \omega_2 t) + \\
 & \quad \cos (\omega_1 t - \omega_2 t) \}
 \end{aligned}$$

since  $\cos 2A = 2 \cos^2 A - 1$  and  $\cos^2 A = \frac{1}{2} \{ \cos 2A + 1 \}$

$$\begin{aligned}
 V = & RI_1 \cos \omega_1 t + \frac{1}{2} A_2 I_1^2 \{ \cos 2\omega_1 t + 1 \} \\
 & + RI_2 \cos \omega_2 t + \frac{1}{2} A_2 I_2^2 \{ \cos 2\omega_2 t + 1 \} \\
 & + A_2 I_1 I_2 \{ \cos (\omega_1 t + \omega_2 t) + \cos (\omega_1 t - \omega_2 t) \}
 \end{aligned}$$

$$\begin{aligned}
V &= R\{I_1 \cos \omega_1 t + I_2 \cos \omega_2 t\} \\
&+ A_2 \{I_1^2 (\frac{1}{2} + \frac{1}{2} \cos 2\omega_1 t) + I_1 I_2 (\cos (\omega_1 t + \omega_2 t) \\
&\quad + \cos (\omega_1 t - \omega_2 t)) + I_2^2 (\frac{1}{2} + \frac{1}{2} \cos 2\omega_2 t)\} \\
&= RI_1 \cos \omega_1 t + RI_2 \cos \omega_2 t \\
&+ \frac{1}{2} A_2 I_1^2 \cos 2\omega_1 t + \frac{1}{2} A_2 I_2^2 \cos 2\omega_2 t \\
&+ A_2 I_1 I_2 \cos (\omega_1 t + \omega_2 t) + A_2 I_1 I_2 \cos (\omega_1 t - \omega_2 t) \\
&\quad + \frac{1}{2} A_2 (I_1^2 + I_2^2)
\end{aligned} \tag{30}$$

Expanding the cube and linear term of Equation 29

$$\begin{aligned}
V &= R(I_1 \cos \omega_1 t + I_2 \cos \omega_2 t) \\
&+ A_3 \{I_1^3 \cos^3 \omega_1 t + I_2^3 \cos^3 \omega_2 t \\
&\quad + 3I_1^2 I_2 \cos^2 \omega_1 t \cos \omega_2 t \\
&\quad + 3 I_1 I_2^2 \cos \omega_1 t \cos^2 \omega_2 t\} \\
&= R(I_1 \cos \omega_1 t + I_2 \cos \omega_2 t) \\
&+ A_3 \{ \frac{1}{4} I_1^3 (\cos 3\omega_1 t + 3 \cos \omega_1 t) + \frac{1}{4} I_2^3 \\
&\quad (\cos 3\omega_2 t + 3 \cos \omega_2 t) \\
&+ \frac{3}{2} I_1^2 I_2 \cos \omega_2 t (\cos 2\omega_1 t + 1) \\
&+ \frac{3}{2} I_1 I_2^2 \cos \omega_1 t (\cos 2\omega_2 t + 1) \}
\end{aligned}$$

$$\begin{aligned}
&= R \{ I_1 \cos \omega_1 t + I_2 \cos \omega_2 t \} \\
&\quad + A_3 \left\{ \frac{1}{4} I_1^3 \cos 3\omega_1 t + \frac{1}{4} I_2^3 \cos 3\omega_2 t \right. \\
&\quad\quad + \frac{3}{4} I_1^3 \cos \omega_1 t + \frac{3}{4} I_2^3 \cos \omega_2 t \\
&\quad\quad + \frac{3}{2} I_1 I_2 \{ I_1 + I_2 \} \\
&\quad\quad + \frac{3}{2} I_1^2 I_2 \cos 2\omega_1 t \cos \omega_2 t \\
&\quad\quad \left. + \frac{3}{2} I_1 I_2^2 \cos \omega_1 t \cos 2\omega_2 t \right\}
\end{aligned}$$

The last two lines can be rewritten

$$\begin{aligned}
&\frac{3}{4} I_1^2 I_2 (\cos (2\omega_1 t + \omega_2 t) + \cos (2\omega_1 t - \omega_2 t)) \\
\text{and} \quad &\frac{3}{4} I_1 I_2^2 (\cos (\omega_1 t + 2\omega_2 t) + \cos (\omega_1 t - 2\omega_2 t))
\end{aligned}$$

== (31)

## BIBLIOGRAPHY

ANDERSON, L.A. and KELLER, G.V., 1964. "A Study in Induced Polarization", *Geop.* Vol. 29, No.5, pp. 848-864.

COLLETT, L.S. and KATSUBE, T.J., 1973. "Electrical Parameters of Rocks in Developing Geophysical Techniques", *Geop.* Vol. 38, No.1, pp. 76-91.

DEKKER, A.J., 1961. "Electrical Engineering Materials", Prentice-Hall Electrical Engineering Series.

FINZI-CONTINI, G. and SOLANI, S., 1969. "A Theoretical Model of Non-linear Phenomena related to Induced Polarization", *Linceri-Rend. Sc. fis. mat. e nat.* Vol. LxVI, pp. 719-724.

FRASER, D.C., KEEVIL, N.B. and WARD, S.H., 1964. "Conductivity Spectra of Rocks from the Craigmont Ore Environment", *Geop.* Vol. 29, No.5, pp. 832-847.

KATSUBE, T.J. and COLLETT, L.S., 1973. "Electrical Characteristic Differentiation of Sulphide Minerals by Laboratory Techniques", 43 *Ann. Inter. S.E.G. Mexico*.

KATSUBE, T.J. and COLLETT, L.S., 1973. "Electrical Characteristics of Rocks and their Application to Planetary and Terrestrial E-M Soundings". *Proceedings of Fourth Lunar Science Conference Supplement Geochemica et Cosmochemica Acta* Vol. 3, pp. 3111-3131

KATSUBE, T.J. and COLLETT, L.S., 1972. "Electrical and E.M. Propagation Characteristics of Igneous Rocks". Paper given at 42<sup>nd</sup> Annual S.E.G. Meeting, California.

KATSUBE, T.J. and COLLETT, L.S. and AHRENS, R.H., 1973. "Electrical Non-linear Phenomena in Rocks", *Geop.* Vol. 38, No.1, pp. 106- 124.

KELLER, G.V. and FRISCHKNECHT, F.C., 1966. "Electrical Methods in Geophysical Prospecting". Pergamon Press, Oxford, p. 517

KELLER, G.V. and LICASTRO, P.H., 1959. "Dielectric Constant and Electrical Resistivity of Natural State" Cores." *Exp. and Theo. Geop. U.S. Geol. Survey Bulletin.* 1052H.

KITTEL, C., 1968. "Introduction to Solid State Physics", John Wiley and Sons, pp. 251- 332.

MADDEN, T.R., 1961. "Electrode Polarization and its influence on the electrical properties of mineralized rocks". Unpublished Ph.D. thesis, M.I.T.

MADDEN, T.R. and MARSHALL, D.J., 1959. "Electrode and Membrane polarisation". U.S./AEC Report R.M.E. - 3157.

MARSHALL, D.J. and MADDEN, T.R. 1959. "Induced Polarization - A Study of its causes". Geop. Vol. 14 No. pp.790-816.

McEUEEN, R.B., BERG, J.W., COOK, K.L., 1959. "Electrical Properties of Synthetic Metalliferous Ore". Geop. Vol. 24, No.3, pp. 510-530

PARKHOMENKO, E.I., 1967. "Electrical Properties of Rocks", Plenum Press N.Y. 1967.

PATTERSON, W.R. and KUHN, M., 1969. "An Electronic System for measuring the Electrical Characteristics of Non-linear devices". Rev. of Sc. Inst

SCOTT, J.H., CARROLL, R.D., CUNNINGHAM, D.R., 1967. "Dielectric Constant and Electrical Conductivity Measurement of Moist Rock". A new laboratory method. J.G.R. Vol 72, No. 20, pp. 5101-5115

SHAUB, Y.B., 1965. "Use of the Non-linear Conductivity Effect in Rocks for Electrical Prospecting". Bull (IZV.) Acad. Sci. USSR, Earth Physics. No.6, pp. 76-81

SHAUB, Y.B., 1969. "Use of the Effects of Nonlinear Electrical Conductivity in the Detection of Disseminated Sulphide Ores". Bull. (IZV.) Acad. Sci. USSR, Earth Physics, No.1, pp. 89-94

SHAUB, Y.B. and IVANOV, V.A., 1971(a) "Experimental Discrimination of Sulphide ores and Graphites by the Use of the Effects of Non-linear Electrical Conductivity". Bull. (IZV.) Acad. Sci. USSR, Earth Physics, No.3, pp. 101-104

SHAUB, Y.B., IVANOV, V.A. and ODINTSOV, V.G., 1971(b) "Model Studies of the Problem of Nonlinear Electrical Prospecting". Bull. (IZV.) Acad. Sci. USSR, Earth Physics, No.4, pp. 94-97

SHAUB, Y.B., IVANOV, V.A. and ODINTSOV, V.G., 1971(c) "Observation of Effects of Non-linear Electrical Conductivity in Boreholes". Bull. (IZV). Acad. Sci. USSR, Earth Physics, No.8, pp. 92-94.

STILL, W.R., 1963. "Noise in Electrode Systems". M.Sc. Thesis, M.T.T. (Unpublished)

SKOV, C.E. and PEARLSTEIN, E. 1964. "Sensitive Method for the Measurement of Non-linearity of Electrical Conduction". Rev. Sc. Inst. Vol. 35, No.8, pp. 962-964

SKOV, C.E. and PEARLSTEIN, E. 1965. "Non-linear Ionic Conductivity in Alkali-Halide crystals". Phy. Rev. Vol. 137, No. SA, pp. 1483- 1494.

SMITH, R.A., 1959. "Semi-conductors". Cambridge University Press.

VALAEU, K.A. and PARKHOMENKO, E.I., 1965. "Electrical Properties of Rocks in Constant and A.C. Fields". Academy of Sciences, USSR, Institute of Physics of the Earth.

VAN VOORHIS, G.D., NELSON, P.H. and DRAKE, T.L., 1973. "Complex Resistivity Spectra of Porphyry Copper Mineralization". Geop. Vol. 38, No.1, pp. 49-60

WARBURG , Von F., 1899. "Ueber das Verhalten Sogenannter Unpolarisirbarer Electroden Gegen Wechselstrom". Annalen der Physik und Chemie, Vol. 67, pp. 493-499

WARBURG , Von F., 1901. "Ueber die Polarisationscapacitat des Platins". Annalen Der Physik und Chemie, Vol.76, pp. 125-135

WARD, S.H. and FRASER, D.C., 1967. "Conduction of Electricity in Rocks". S.E.G. Mining Geophysics, Vol. 2.